Miltefosine increased cholesterol efflux, induced autophagy and inhibited NLRP3-inflammasome assembly and IL-1β release.

Iacano: Miltefosine inhibits Nlrp3 inflammasome and IL-1β release.

Amanda J Iacano[1], Harvey Lewis[1], Jennie E Hazen[1], Heather Andro[1], Gregory Brubaker[1], Bani A Raheem[1], Jonathan D Smith[1,2*], and Kailash Gulshan[1*]

[1]Department of Cellular and Molecular Medicine, Cleveland Clinic, Cleveland OH 44195, USA.
[2]Department of Cardiovascular Medicine, Cleveland Clinic, Cleveland OH 44195, USA.

Total Word count: 10349
Word count of abstract: 263
Numbers of figures and tables: 7

*Correspondence to: Kailash Gulshan, Ph.D., Department of Cellular and Molecular Medicine, Cleveland Clinic, Cleveland OH , 9500 Euclid Avenue, Box NC10 Cleveland, OH 44195, Phone: 216-445-3699), Email: gulshak@ccf.org or Jonathan D. Smith, PhD, Department of Cellular and Molecular Medicine, Cleveland Clinic, 9500 Euclid Ave, Box NC10, Cleveland, OH 44195, Email: smithj4@ccf.org.

Key Words: Cholesterol efflux, Abca1, p62, LC3, Autophagy, Miltefosine, Nlrp3 Inflammasome, IL-1β.

Abstract: In advanced human plaques and aged patients, athero-protective pathways such as autophagy and reverse cholesterol transport (RCT) become dysfunctional, while atherogenic pathways such as NLRP3 inflammasome and TLR2/4 are induced. Here, we report that Miltefosine, an FDA approved drug for treating leishmaniasis, increased cholesterol efflux, induced membrane remodeling, and induced autophagy in macrophages. Macrophages treated with Miltefosine exhibited markedly increased ABCA1 mediated cholesterol efflux and decreased phosphatidylserine flip from the cell-surface. Miltefosine treatment of macrophages led to redistribution of phosphatidylinositol 4,5-bisphosphate (PIP2) from plasma membrane to actin rich regions of the cell. RAW264.7 macrophages treated with Miltefosine showed marked increase in p62 and LC3 puncta staining vs. control cells. The Lipid droplet degradation was induced by Miltefosine leading to ~ 50% decrease in the CE:FC (cholesterol ester: free cholesterol) ratio. The TLR4 signaling pathway in LPS primed bone marrow derived macrophages was blunted by Miltefosine treatment, leading to ~75% reduction in pro-IL-1β mRNA levels. Miltefosine pretreatment of macrophages potently inhibited NLRP3 inflammasome assembly induced by LPS/ATP treatment, exhibiting ~70% reduction in ASC1 speck forming cells. Gasdermin D mediated release of mature IL-1β was reduced by ~80% in Miltefosine treated vs. control cells. The qRT-PCR and western blot analysis showed no changes in basal or LPS induced levels of inflammasome components (NLRP3, ASC1, procaspase1), while the LPS mediated induction in ROS levels was significantly blunted in Miltefosine treated vs. control macrophages. Miltefosine did not alter the AIM2 inflammasome activity indicating specific targeting of Nlrp3 inflammasome pathway. Overall, this study showed that Miltefosine targets lipid trafficking, cell migration, autophagy, and Nlrp3 inflammasome activity in macrophages.

Non-standard abbreviations and acronyms:

AMPK, AMP-activated protein kinase
apoA1, apolipoprotein A-I
apoE, apolipoprotein E
ABCA1, ATP-binding cassette transporter A1
ASC1, apoptosis-associated speck protein containing a CARD (Caspase activation and recruitment domain)
DMPC, 1,2-dimyristoyl-sn-glycero-3-phosphatidylcholine
Gsdmd; Gasdermin D
HDL-C, high-density lipoprotein-cholesterol
IL1-β, Interleukin 1-beta
LXR, liver X receptor
NLRP3, NOD-like receptor family pyrin domain-containing 3
NF-kB, nuclear factor kappa-light-chain-enhancer of activated B cells
PS, phosphatidylserine
PC, phosphatidylcholine
POPS, 1-palmitoyl-2-oleoyl-sn-glycero-3-serine
SR-BI, scavenger receptor-BI
TLR, toll like receptor

Significance Statement:

Atherosclerosis is a progressive inflammatory disease. In advanced human plaques, the athero-protective pathways such as reverse cholesterol transport (RCT) and autophagy become increasingly dysfunctional while atherogenic pathways such as NLRP3 inflammasome are aberrantly induced. The cholesterol efflux via RCT prevents atherosclerosis and inflammation by reducing lipid loads in foam cells. Autophagy, in addition to playing a pivotal role in removing stored cholesterol from macrophages, promotes removal of inflammasome activating stimuli from cytosol (such as damaged mitochondria), thus helping in sequestering IL-1β. Failure of foam cells to egress from plaques and prolific engulfment of modified lipids results in formation of cholesterol crystals, leading to induction of NLRP3 inflammasome assembly. The release of IL-1β from foam cells further amplify the inflammation and promote further infiltration of immune cells to plaque. How RCT, autophagy, and inflammation pathways coordinate with each other to maintain cellular homeostasis is not clear; thus, the interplay between these pathways needs to be investigated thoroughly. Increased cholesterol efflux and induced autophagy with simultaneous dampening of Nlrp3 inflammasome can prevent atherosclerosis. Here, we show that Miltefosine can target multiple pathways involved in lipid homeostasis and inflammation. The detailed investigation of mechanisms involved in Miltefosine's action may led to novel therapeutic targets for preventing and treating atherosclerosis and CVD.

Introduction: Based on the American Heart Association's 2016 Heart Disease and Stroke Statistics update; heart disease and stroke were the No. 1 and No. 2 killer worldwide[23]. Atherosclerosis, a sterile inflammatory disease, is the driving force behind progression of Coronary artery disease (CAD) and cardiovascular disease (CVD). The excess levels of low-density lipoproteins (LDLs) in blood can be deposited and modified in arterial intima, where macrophages can uptake these lipids. The continuous uptake of toxic lipids and failure of macrophages to regress results in foam cell formation. The foam cells over time can become dysfunctional and undergo necrosis, leading to increased recruitment of immune cells to plaque area[1]. Accumulation of cholesterol crystals and oxidized lipids in plaques can also activate NLRP3 inflammasome to further promote atherosclerosis[2, 3]. The NLRP3 inflammasome is reported to be activated in aortas of advanced atherosclerosis patients as well as in other metabolic diseases such as obesity[4 5, 6]. The NLRP3 inflammasome plays a role in processing procaspase 1 resulting in subsequent caspase 1 mediated processing of pro IL-1β to generate active Interleukin-1β (IL-1β). The role of IL-1β in promoting human CVD was highlighted by the recently concluded Cantos trial, showing that anti-IL-1β therapy met the primary trial endpoint, *a* reduction in a composite of heart attack, stroke and cardiovascular death[7]. A newly discovered substrate of caspase1 and caspase 11, Gasdermin D, plays an essential role in pyroptosis (necrotic cell death) and IL-1β release [8-10]. Gasdermin D is also necessary for IL-1β release following LPS and nigericin treatment under conditions that prevented cell membrane rupture[11]. Modified cholesterol promotes recruitment of Toll-like receptors 2 and 4 (TLR2/TLR4) to plasma membrane of foam cells, leading to activation of NF-kB signaling and increased synthesis of pro IL-1β mRNA transcript. Circulating monocytes from human patients with atherosclerosis exhibit increased expression of TLR2/4 and Apo $E^{-/-}$ null mice carrying large plaque burden displayed increased surface expression of TLR2 and

TLR4 on circulating monocytes[12]. The induction of TLR (for production of IL-1β mRNA) and NLRP3 (for processing and release of IL-1β) in advanced atherosclerotic plaques can lead to amplification of immune responses and plaque instability. In contrast to atherogenic pathways, the atheroprotective pathways such as autophagy and cholesterol efflux become increasingly dysfunctional in advanced atherosclerotic plaques, aged patients, and in arteries of atherosclerosis and diabetes animal models[3, 13, 14]. During lipid-droplet autophagy, lipid droplets are engulfed by autophagosomes that then fuse with lysosomes where cholesterol esters are hydrolyzed to generate free cholesterol [13, 14]. Many lines of evidence have shown that inhibition of autophagy by drugs or genetic methods is associated with increased atherosclerotic plaque burden[3, 13, 15]. Once the free cholesterol is generated by lipid-droplet autophagy it can be transported back to liver for excretion via reverse cholesterol transport (RCT) [16-20]. In addition to removing cholesterol, Abca1 expression can also disrupt lipid-rafts and dampen TLR recruitment to cell membrane[21]. Thus, the simultaneous induction of athero-protective pathways, such as cholesterol efflux and autophagy, along with dampening of athero-promotive pathways such as TLR signaling and Nlrp3 inflammasome assembly, may serve as a novel therapeutic treatment for CVD patients. Here, we report that Miltefosine, an FDA approved drug for treating visceral and cutaneous leishmaniasis, promoted cholesterol efflux, disrupted lipid-rafts and TLR4 signaling, increased cell-surface PS exposure, induced PIP2 trafficking from PM to cell periphery, induced basal autophagy, reduced LPS induced mitochondrial ROS generation and blunted NLRP3 inflammasome assembly and IL-1β release.

Results:

Miltefosine induced Abca1 mediated cholesterol efflux from cells. Previous study have shown that Miltefosine and other alkylphospholipids induces cholesterol efflux from the HepG2 cells[22]. We tested effect of Miltefosine treatment on cholesterol efflux in RAW 264.7 macrophages. The RAW264.7 macrophages were radiolabeled with tritium cholesterol and induced with 8Br-cAMP to induce Abca1 expression. The control and ABCA1 expressing cells were incubated with different doses of Miltefosine for 1h or 4h and cholesterol efflux was determined. As shown in ***Fig. 1A***, the Miltefosine treatment of control RAW cells led to ~1.45% increase (with 7.5μM Miltefosine) in cholesterol efflux to media (with ANOVA, mean± SD, n=6, $p<0.05$) and ~3.1% increase with 10μM Miltefosine (with ANOVA, mean± SD, n=6, $p<0.005$). The RAW cells induced for Abca1 expression showed much more robust cholesterol efflux to media in presence of Miltefosine with ~5.0 % increase with 7.5μM Miltefosine treatment (with ANOVA, mean± SD, n=6, $p<0.05$) and ~10 % increase in cholesterol efflux to media with 10 μM Miltefosine treatment (with ANOVA, mean± SD, n=6, $p<0.005$). To test the specificity of Miltefosine in inducing Abca1 mediated cholesterol efflux, we used Abca1 expressing non-macrophage HEK293 and BHK cell lines. In both cases, addition of Miltefosine markedly increased Abca1 mediated cholesterol efflux to the media in absence of any cholesterol acceptor (***Fig. S1, S2***). During 1h chase period with Miltefosine, the addition of cholesterol acceptor apoA1 further increased cholesterol efflux with Abca1+apoA1+7.5 μM Miltefosine treated cells vs. Abca1+apoA1 cells showing~4.8 % increase (with ANOVA, mean± SD, n=6, $p<0.005$) and Abca1+apoA1+10 μM Miltefosine treated cells vs. Abca1+apoA1 cells showing ~6.45 % increase in cholesterol efflux (with ANOVA, mean± SD, n=6, $p<0.005$). (***Fig 1A***). At higher concentration of 10μM Miltefosine and during 6h chase time period, the Abca1 mediated cholesterol efflux to media was more than efflux to apoA1 (***Fig 1A, S3***), indicating

that Miltefosine may promotes ABCA1 mediated cholesterol efflux via microparticle generation in an acceptor independent manner. To determine the mechanism by which Miltefosine increased cholesterol efflux via Abca1, we performed western blot analysis of the total and cell-surface Abca1 levels. RAW264.7 macrophages were treated cAMP to induce Abca1 expression, followed by treatment with ± 7.5 μM Miltefosine for 4h and cell extract preparation for total and cell-surface protein fractions and western blot analysis. As shown in ***Fig.1B***, no significant increase was observed in either total or cell-surface Abca1 expression levels in control vs. Miltefosine treated cells, indicating that Miltefosine induced cholesterol efflux is not due to increased Abca1 levels. We also tested if Miltefosine affected apoA1 cellular binding by performing a flow-cytometry based assay using Alexa-647 labeled apoA1 as described in earlier study[23]. RAW cells ± ABCA1 expression were incubated with Alexa-647 labeled apoA1 for 45 min at 37^0C ± 7.5μM Miltefosine. As expected, Abca1 expressing cells showed increased Alexa-647 apoA1 binding, while no significant differences were observed in apoA1 cell membrane binding in Miltefosine treated vs. non treated RAW264.7 macrophages (***Fig. 1C***). Next, we tested if Miltefosine modulated apoA1 mediated lipid-solubilization. ApoA1 in lipid-free form can spontaneously interact with DMPC liposomes and solubilize them, resulting in decreased turbidity of the liposome suspension, and generation of reconstituted HDL (rHDL). We performed apoA1 mediated liposome clearance assays at room temperature, using liposomes constituted of either DMPC alone or DMPC liposomes containing 5% Miltefosine. As shown in ***Fig. 1D***, Miltefosine markedly enhanced the DMPC clearance by lipid-free apoA1. To further probe the role of Miltefosine in mediating enhanced cholesterol extractability from membranes that are more physiological and have similar lipid profile as plasma membrane, we performed lipid-solubilization assays using liposomes comprised of POPC, cholesterol and, PS. The POPC:PS:cholesterol MLVs were previously shown to be

slowly solubilized by apoA1 at acidic pH [24]. The addition of 5% Miltefosine to POPC:Cho:PS liposomes further increased rate of liposome clearance by apoA1 at lower pH (***Fig 1E***). Next, we tested Miltefosine analogues as well as lyso-PC for apoA1 mediated lipid solubilization. Perifosine and edelfosine promoted apoA1 mediated lipid solubilization at rate either equal or higher than Miltefosine while the lyso-PC also increased lipid solubilization by apoA1 but at lower rate than Miltefosine ***(Fig S4)***. These data indicated that Miltefosine promoted structural changes in lipid membrane that may facilitate the apoA1 mediated liposome solubilization.

Miltefosine increased PS exposure by inhibiting PS flip in macrophages: Lipid rafts are comprised mainly of PC, cholesterol and sphingomyelin[25]. Disruption of lipid-rafts by Abca1 is proposed to provide free cholesterol pool for efflux and hamper TLR signaling pathway via reduced recruitment of TLR2/4 to lipid-rafts[26 21, 27]. Previous studies have also shown that Miltefosine use lipid-rafts as entry portals to cells[28] and can also act as an lipid-raft disrupting agent to inhibit human mast cell activation[29]. We determined the status of lipid-rafts in Miltefosine treated RAW264.7 macrophages by staining for the ganglioside GM1 with Alexa 647-labeled cholera toxin B, followed by either fluorescent microscopy or flow cytometry. As shown in ***Fig. 2A***, RAW 264.7 macrophages treated with ± 7.5 μM Miltefosine for 16h displayed remarkably lower GM1-CTB staining as observed by fluorescent microscopy, indicating disruption of lipid-rafts. For quantification of lipid-rafts, the flow-cytometry based binding analysis of cells treated with ± 7.5 μM Miltefosine for 16h was carried out using Alexa-647 labeled CTB. The Miltefosine treated cells showed ~26% less binding as compared to control cells (with two tailed t-test, mean± SD, n=3, $p<0.004$) (***Fig. 2B***). Disruption of lipid rafts may increase the availability of cholesterol at plasma membrane. In addition, other mechanisms such as disruption in cholesterol trafficking from plasma membrane to endoplasmic reticulum can also increase cholesterol on plasma membrane[30]. We have

previously shown that membrane remodeling resulting in lipid raft disruption can also increase cell-surface PS, that can promote cholesterol extraction from cell membrane[23]. We investigated if Miltefosine increased PS exposure at the cell-surface by performing a flow-cytometry based Annexin Cy5 binding assay. Cells expressing Abca1 were used as positive control as PS exposure is increased by Abca1 PS floppase activity[31, 32]. As shown in ***Fig. 2C***, cells treated with 7.5μM Miltefosine for 16h showed increased PS exposure at cell surface. The cells without Abca1 expression showed ~24% increase in PS exposure vs. control cells with ANOVA, mean± SD, n=4, $p<0.005$. The cells expressing Abca1 showed increased PS exposure (~23% vs control increase with ANOVA, mean± SD, n=4, $p<0.05$). The PS exposure was further increased in Abca1 expressing cells treated with Miltefosine (~39% increase vs. control with ANOVA, mean± SD, n=4, $p<0.0005$). We have previously shown that the incremental increased PS exposure observed upon Abca1 expression is well below than PS exposure observed in cells undergoing apoptosis[23]. These data indicated that Miltefosine increased PS exposure by a mechanism different than increased Abca1 mediated PS flop from inner leaflet to the outer leaflet of plasma membrane. The increased levels of cell surface PS upon Miltefosine treatment could be due to decreased rate of PS flipping (inward translocation). To qualitatively observe the PS flipping across plasma membrane by fluorescent microscopy, we used head-group labeled NBD-PS. Control RAW264.7 cells and cells treated with 7.5uM Miltefosine for 16h were incubated with exogenously added NBD-PS. In control cells, majority of the exogenous NBD-PS moved to intracellular compartments over a 15 min incubation period at 37^{o}C (**Fig. 2D**). However, in Miltefosine treated cells, much less NBD-PS was observed inside the cells. To quantitatively measure flipping of NBD-PS, we used a previously described flow-cytometry based method using membrane-impermeable NBD quenching reagent sodium dithionite[23]. RAW cells treated with ± 7.5uM Miltefosine for 16h

were incubated with NBD-PS for 15 min at 37 °C, sodium dithionite was added to selected aliquots, followed by flow cytometry analysis. The amount of NBD-PS flipped into the cells was calculated by measuring the % of NBD fluorescence resistant to quenching by sodium dithionite. As shown in ***Fig. 2E***, Miltefosine treated cells flipped significantly lower amounts of NBD-PS as compared to control cells (~44% vs. ~70% by ANOVA, mean± SD, n=4, $p<0.0002$). These data indicated that Miltefosine inhibited PS flip from the cell surface, resulting in increased PS exposure at the plasma membrane.

PIP2 is redistributed from plasma membrane upon Miltefosine treatment. Similar to PS, PIP2 is also sequestered to inner leaflet of PM. To determine the effect of Miltefosine on PIP2 trafficking and localization, RAW264.7 cells stably transfected with plasmid containing 2X-PH-PLC-eGFP construct were treated with ± 7.5 μM Miltefosine for 16h. The cells were washed with serum free media and PIP2 reporter localization was determined by fluorescent microscopy. As shown in ***Fig. 3A***, control cells showed uniform localization of PH-PLC-eGFP at the plasma membrane while the cells treated with Miltefosine showed delocalization of PIP2 from plasma membrane and enrichment at cytoplasm near the periphery of cells. This kind of PIP2 enrichment is usually observed in cells undergoing migration, where actin and PIP2 shifts towards the back of migrating cells. To test the colocalization of PIP2 and actin, RAW264.7 cells treated with7.5 μM Miltefosine for 16h were fixed, permeabilized and incubated with beta-actin antibody, followed by counterstaining with Alexa 568 labeled goat anti-mouse antibody and fluorescent microscopy. As shown in ***Fig. 3B***, PIP2 reporter GFP signal colocalized with beta actin, indicating that Miltefosine may be promoting cell migration in macrophages.

Miltefosine induced basal and lipid-droplet autophagy. Autophagy plays a protective role in atherosclerosis[14] and it is impaired in advanced human plaques[13]. Autophagy is required for degradation of lipid-droplets in foam cells and generating free cholesterol from cholesterol

esters for efflux from the cells. Given that Miltefosine increased cholesterol efflux from the cells, we speculated that Miltefosine may induced autophagy of cholesterol esters to generate free cholesterol. Upon autophagy induction, the cytosolic form of LC3 (LC3-I) is conjugated to phosphatidylethanolamine to form lipidated LC3-II. The PE-conjugated LC3-II is recruited to autophagosome membrane and can be observed as cytoplasmic puncta by microscopy while the adaptor protein p62 is responsible for chaperoning damaged proteins and organelles to autophagophore. To test if Miltefosine can induce autophagy in macrophages, we probed the RAW 264.7 macrophages treated with ± 7.5 μM Miltefosine for 16h with autophagy markers LC3 and p62. The Miltefosine treated cells showed multiple p62 puncta in cytoplasm, while control cells had evenly distributed weak cytoplasmic signal with almost no p62 puncta signal (***Fig. 4A,*** upper panel). Miltefosine treatment also increased lipidated form of LC3-II as observed by puncta formation in macrophages transfected with LC3-GFP plasmid and by microscopy (***Fig. 4A*** lower panel). Next, we evaluated whether the LC3 puncta was due to increased autophagic initiation or due to decreased autophagic flux leading to an accumulation of autophagic markers. The levels of LC3-II were determined by western blotting in presence of chloroquine. Chloroquine inhibits the autophagic flux leading to accumulation of LC3-II. Western blot analysis of LC3-II showed that the LC3-II protein levels were increased by 4.3-fold in Miltefosine cells vs. control cells (***Fig.4B, 4C***), while there was a 3.1 fold increase in Miltefosine + chloroquine cells as compared to cells treated with chloroquine alone. These data indicated that Miltefosine induced autophagy and had no effect on autophagic degradative flux. Next, we tested if autophagy induced by Miltefosine could degrade cholesterol ester rich lipid droplets to generate free cholesterol for efflux. RAW264.7 macrophages were cholesterol loaded by incubation with 100 μg/ml acetylated LDL (AcLDL) for 24h to generate foam cells. These foam cells were then treated with ± 7.5 μM Miltefosine and ± acat inhibitor (Acati) for 4h.

Aacti prevents the esterification of free cholesterol to cholesterol esters. The total and free cholesterol levels were determined by enzymatic assay described previously[33]. As expected, the AcLdL loaded cells had higher ratio of cholesterol ester to free cholesterol (***Fig. 4D***). The cells treated with actai had higher free cholesterol levels and thus lower CE::FC ratio, while the Miltefosine treated cells showed further lowering of CE::FC ratio, indicating increased levels of free cholesterol. This data indicated that Miltefosine can induce degradation of lipid-droplets generating free cholesterol (***Fig. 4D***). To decipher the mechanism by which Miltefosine was inducing lipid droplet degradation in macrophages, we determine the phosphorylation status of AMPK in control vs Miltefosine treated cells. AMPK phosphorylation is known to induce autophagy RAW264.7 macrophages loaded with 100μg/ml AcLdL were treated with 7.5μM Miltefosine for 4h followed by cell extracts preparations. As shown in ***Fig. 4E***, AMPK phosphorylation levels were higher in Miltefosine treated macrophages.

Miltefosine decreased LPS mediated induction in IL-1β levels Lipid-rafts plays an essential role in AKT signaling, TLR2/4 signaling pathway and atherosclerosis progression[21, 27, 34-36]. TLR4 activation leads to plasma membrane recruitment of MyD88, followed by phosphorylation of downstream kinases such as IkappaB Kinase alpha (IKBα) and NF-kB nuclear translocation. Since Miltefosine treatment led to lipid-raft disruption, we investigated status of TLR4 signaling pathway in Miltefosine treated bone-marrow derived macrophages (BMDMs). Control and Miltefosine pretreated BMDMs were incubated with 1μg/ml LPS for 30 min, followed by western blot analysis of phosphorylated form of IKBα. A shown in ***Fig. 5A***, the LPS mediated increase in phosphorylation of IKBα was reduced in Miltefosine treated cells. To determine the levels of NF-kB translocating inside the nucleus, macrophages were treated with LPS for 30 min, followed by fixing the cells, probing with anti-NF-kB antibody and Alexa-568 labeled anti-rabbit secondary antibody and imaging using fluorescent microscopy. The

Miltefosine treated cells showed reduced NF-kB translocation inside the nucleus vs. control cells (***Fig. 5B***). Next, we tested if LPS mediated synthesis of pro IL-1β messenger RNA was affected by Miltefosine by performing a qRT-PCR analysis using IL-1β specific primers and control actin b primers. As expected, the mRNA levels of pro IL-1β were significantly induced in LPS treated control cells as compared to cells not treated with LPS (***Fig. 5C***). Though the LPS induced increase in levels of IL-1β levels were observed in both control and Miltefosine treated BMDMs, the Miltefosine pretreated macrophages showed ~4.5 fold decrease in mRNA levels of pro-IL-1β (with two tailed t-test, mean± SD, n=3, $p<0.034$) (***Fig. 5C).*** Next, we performed western blot analysis of protein levels of pro IL-1β in control vs. Miltefosine treated cells. A shown in ***Fig. 5D***, the LPS mediated induction in pro IL-1β protein levels was decreased in Miltefosine treated cells. Taken together, these data indicated that Miltefosine disrupted lipid-rafts, dampened TLR signaling pathway and decreased the LPS mediated induction in IL-1β mRNA and protein levels in macrophages.

Miltefosine inhibited NLRP3 inflammasome assembly and IL-1β release: Cholesterol crystals can cause disrupt autophagolysosome membrane, leading to NLRP3 inflammasome assembly[2, 37]. We tested effects of Miltefosine treatment on inflammasome assembly and IL-1β release in bone-marrow derived macrophages. Control and BMDMs pretreated with 5μM Miltefosine for 16h, were primed with LPS for 4h and incubated with ATP for 20 min, followed by probing with anti-ASC1 antibody for visualization of Nlrp3 inflammasome assembly or IL-1β ELISA. The BMDMs pretreated with Miltefosine showed remarkably decreased Asc1 specks formation upon LPS+ATP stimulation (~40% as compared to 12% in control vs. Miltefosine treated cells (***Fig.6A, 6B, S5, S6***). Next, we performed IL-1β ELISA on media obtained from control and Miltefosine treated macrophages and found that cells treated with Miltefosine had ~80% decreased IL-1β release as compared to control macrophages (with two tailed t-test,

mean± SD, n=3, p<0.0039) (***Fig.6C***). To decipher the mechanism by which Miltefosine is preventing Nlrp3 inflammasome assembly, we determined the mRNA and protein levels of various Nlrp3 inflammasome complex members in BMDMs with or without LPS priming. The qPCR analysis was performed on control and Miltefosine pretreated BMDMs using actin b as control. The LPS mediated increase in transcript levels of, NLRP3 (3.34 fold increase in LPS treated and 3.36 fold increase in LPS+ Miltefosine treated cells by ANOVA, mean± SD, n=4, p<0.0001), procaspase 1 (2.74 fold increase in LPS treated and 3.31 fold increase in LPS+ Miltefosine treated cells by ANOVA, mean± SD, n=3, p<0.0001), and Gasdermin D (1.3 fold increase in LPS treated and 2.25 fold increase in LPS+ Miltefosine treated cells by ANOVA, mean± SD, n=4, p<0.0001), were observed(***Fig. 6D***). These data indicated that Miltefosine treatment did not affect the transcription of these genes. In agreement with earlier published studies[38], the western blot analysis showed robust induction in protein levels of NLRP3 upon LPS treatment (***Fig. 6E)***, while there was no change in protein levels of Asc1 or procaspase 1 ***(Fig. 6F, 6G)***. The release of mature IL-1β from cells is regulated by Gasdermin D mediated pore formation on plasma membrane[9, 10]. We tested if Miltefosine effected Gasdermin protein levels or Gasdermin D activity by performing western blot analysis and IL-1β ELISA in control vs. Miltefosine treated BMDMS. There were no alteration in Gsdmd protein levels by Miltefosine treatment (***Fig. S7***). Taken together, these data indicated that Miltefosine dampened the IL-1β release by targeting Nlrp3 inflammasome pathway.

Miltefosine blocks Nlrp3 inflammasome in cholesterol independent manner and reduces mitochondrial ROS. We determined if defects in IL-1β release in Miltefosine treated cells is indeed due to disruption of Nlrp3 inflammasome by using an Nlrp3 specific inhibitor MCC9550. As shown in ***Fig. 7A***, the cells treated with Miltefosine and MCC9550 did not show additive effects on the levels of IL-1β release as compared to cells treated with Miltefosine or MCC590

alone (with ANOVA, mean± SD, n=3, n.s.). Next, to test if Miltefosine specifically inhibited ATP/LPS induced NLRP3 inflammasome assembly and IL-1β release, we tested effects of Miltefosine on AIM2 inflammasome. The control and Miltefosine treated macrophages were primed with LPS (1mg/ml) for 4hrs followed by lipofectamine mediated transfection of poly (dA:dT) for 3h. The media was collected and subjected to IL-1β ELISA and as shown in ***Fig. 7B***, there was no difference in levels of released IL-1β in control vs. Miltefosin treated macrophages (with two tailed -test, mean± SD, n=3, n.s.). These data indicated that Miltefosine did not alter AIM2 inflammasome activity. Previous studies have shown that deficiency of abca1/abcg1 increases inflammation in macrophages and ABCA1 mediated cholesterol efflux in dendritic cells dampen inflammasome assembly [39, 40]. Though we have used cholesterol unloaded BMDMs for inducing inflammasome, there is a possibility that Miltefosine is inhibiting Nlrp3 inflammasome assembly via cholesterol depletion. To directly test the role of cholesterol depletion on Nlrp3 inflammasome assembly, we treated unloaded BMDMs with 5μM Miltefosine for 16h or with 1mM cyclodextrin for 2h at 37^0C, followed by LPS/ATP incubation. As shown in ***Fig. 7C***, the cholesterol levels in BMDMs treated with cyclodextrin were significantly lower as compared to Miltefosine treated cells (with ANOVA, mean± SD, n=3, $p<0.01$), but Miltefosine was much more effective in inhibiting inflammasome activity (***Fig. 7D***) as assayed by ASC1 specks per cell (***Fig. S8***) and mature IL-1β release (with ANOVA, mean± SD, n=3, $p<0.0016$ for control vs. Miltefosine, n.s. for control vs. cyclodextrin). These data indicated that Nlrp3 inhibition by Miltefosine is not solely due to cholesterol depletion.

Since Miltefosine treatment did not alter the expression levels of Nlrp3 inflammasome pathway components such as Nlrp3, Asc1, Caspase 1 or Gasdermin D, we focused on role of mitochondria in Nlrp3 inflammasome assembly. determined the status of mitochondrial ROS ,

Mitochondria plays an important role in induction and assembly of Nlrp3 inflammasome with mitochondrial ROS responsible for driving NLRP3 inflammasome assembly[41] while mitochondrial cardiolipin providing a docking site for Nlrp3 protein binding and inflammasome assembly[42]. We tested the mitochondrial ROS production by staining with MitoSox reagent in control and Miltefosine treated BMDMs with or without LPS treatment. As shown in ***Fig. 7E***, the LPS treatment induced ROS production in cells as evident by increased staining with MitoSox while the Miltefosine pretreated cells showed blunted induction in MitoSox staining upon LPS treatment. To quantify the MitoSox binding, we performed a flow-cytometry based binding assay. A shown in ***Fig. 7F***, Miltefosine treated cells showed significantly reduced binding to MitoSox, indicating decreased levels of LPS mediated ROS generation in Miltefosine treated cells vs. control cells. Collectively, our data suggested that Miltefosine may be preventing Nlrp3 inflammasome assembly by eliminating damaged mitochondria by promoting autophagy and thus reducing ROS levels in cells treated with LPS.

Discussion

Given the multifaceted nature of pathways involved in promoting atherosclerosis and CVD, the drugs that can simultaneously induce atheroprotective pathway and dampens atherogenic pathways may be used as stand-alone or as an adjuvant therapy with current CVD therapies. Miltefosine is on WHO model list of essential medicines and is was approved by FDA in 2014 for treating cutaneous and visceral leishmaniasis. Miltefosine is also used to treat free-living amoeba infections such as Naegleria fowleri[43]. The structure of Miltefosine is similar to lyso-PC and it is known to integrate in the cell membrane and redistribute in intracellular membranes of ER, Golgi and mitochondria. Miltefosine and other similar alkylphospholipids are proposed to perturb phospholipid and sphingolipid homeostasis and also cause a deregulation of cholesterol homeostasis by impairing cholesterol transport from plasma membrane to the ER

[30]. It's important to note that the mechanism of action of Miltefosine, whether regarding killing of parasites or cancer cells, is not completely clear and It is widely believed that most of the downstream effects of Miltefosine are dependent on cell-type with reported range of activities such as induction of apoptosis in cancer cells and inhibition of Mast cell activation[29, 44].

We found that Miltefosine has multiple activities in macrophages; inducing Abca1 mediated cholesterol efflux from cells, promoting lipid-raft disruption, inhibition of PS flip from the cell-surface, redistribution of PIP2 to actin-rich regions indicating induction of cell migration , induction of basal and lipid droplet degradation, and inhibiting NLRP3 inflammasome assembly and IL-1β release. As shown before in HepG2 cells[22], Miltefosine increased the cholesterol efflux from the control RAW264.7 murine macrophages. Interestingly, cells expressing Abca1 effluxed cholesterol at much higher levels to media in the absence of any cholesterol acceptor (***Fig. 1A***), though no significant changes in Abca1 levels were observed in Miltefosine treated vs. control macrophages. Miltefosine can effect plasma membrane fluidity and membrane fluidity plays a role in ABCA1 mediated microparticle generation[45]. Thus combination of Miltefosine and Abca1 may lead to higher cholesterol efflux through release of lipids/cholesterol in form of microparticles. Miltefosine treatment led to disruption of lipid-raft that can increase the plasma membrane pool of free cholesterol and increased PS exposre conferred by Miltefosine can promote cholesterol extraction from the cells. We have shown before that limited increased exposure of PS on cell-surface can promote cholesterol extraction from membranes [23]. The rate of PS flips from outer leaflet of plasma membrane to inner leaflet was decreased in Miltefosine treated cells, indicating that the PS exposure is mostly due to decreased PS flip rather than increased PS flop by Abca1's lipid floppase activity. Previous study have shown that short-term treatment of HePG2 cells with 50 μM Miltefosine and other alkylphospholipids induces cholesterol efflux from the cells to

extracellular media[22] , while prolonged treatment with Miltefosine can cause defects in apoA1 mediated cholesterol efflux in HepG2 and TPA-treated THP1 cells[44]. Though, we did not see significant increase in cholesterol efflux to apoA1 with higher dose of Miltefosine or during longer chase time-periods with Miltefosine, we attribute this effect to robust activation of Abca1 mediated cholesterol efflux to media. We tested and found that apoA1 mediated lipid-solubilization was increased in presence of Miltefosine. At the lipid phase transition temperature, the membrane lattice defects at phase boundaries facilitates the increased rate of solubilization of phospholipid liposomes by apoAI [46]. Miltefosine may increase the packing defects at the phase transition temperature, leading to increased insertion of apoA1 into liposomes.

The lipid-rafts play an essential role in recruiting TLRs to plasma membrane to initiate a signaling cascade that allows cytoplasmic NF-kB to shuttle inside the nucleus and upregulate the transcript levels of pro IL-1β. Resting macrophages express low levels of this genes but macrophages primed with primary signal such as LPS can robustly induce mRNA levels of pro IL-1β as well as NLRP3. Miltefosine treated cells showed significantly lowered levels of LPS induced pro IL-1β transcript levels. Surprisingly, the NLRP3 transcript levels in Miltefosine treated cells were induced similar to untreated cells, though both IL-1β and NLRP3 transcripts are induced by NF-kB. The LPS induced nuclear localization of NF-kB was partially inhibited in Miltefosine treated cells, indicating delayed TLR4 mediated cell signaling rather than a complete blockage. Since the levels of NLRP3 transcripts were modestly increased as compared to robust induction seen in case of pro IL-1β transcript levels, the decreased shuttling of NF-kB may not hinder NLRP3 transcription as compared to IL-1β transcription. Given the sharp decrease in levels of pro IL-1β transcript levels, in addition to decrease

synthesis of mRNA, Miltefosine treatment may also be destabilizing IL-1β mRNA leading to increased degradation of IL-1β transcripts.

Autophagy plays a protective role in atherosclerosis[14] and it is impaired in advanced human plaques[13]. Autophagy is controlled by multiple pathways responding to stimuli such as the status of cellular energy (AMP-dependent protein kinase, AMPK) or amino acid availability (target of rapamycin, TOR). Miltefosine induced basal autophagy in macrophages as evident by increased cytoplasmic p62 and LC3-GFP puncta. Miltefosine treated cells showed increased degradation of cholesterol esters as compared to control cells. The cells treated with ACATi showed higher free cholesterol levels in control cells but the Miltefosine treatment further increased the levels of free cholesterol. This data along with electron microscopy data showing double membrane bound autophagosomes containing *lipid-droplets*, mitochondria, and other organelles, supports the notion that Miltefosine may induce degradation of lipid-droplets via lipophagy. Increased phosphorylation of AMPK observed in Miltefosine treated cells as compared to control cells can explain induced basal autophagy observed in Miltefosine treated cells.

The components of inflammasome complex, NLRP3, ASC1, Caspase1, and, IL1- β are significantly increased in atherosclerotic plaques compared to healthy arteries. Blocking of NLRP3 by a chemical drug MCC9550 reduces atherosclerosis in mouse and infarct size in pigs [47, 48] and recent trials showed the reduced cardiovascular events upon treatment with IL-1β antibodies [7] . The most striking activity of Miltefosine was its ability to strongly block the assembly of Nlrp3 inflammasome upon LPS and ATP stimuli and reduce release of mature IL-1β from macrophages. Nlrp3 inflammasome assembly is controlled via transcriptional as well as via posttranslational mechanisms. The protein levels of NLRP3 are boosted by a non-transcriptional priming pathway, involving TLR4 and Myd88, via NLRP3 deubiquitination[38]. The

basal levels of NLRP3 inflammasome components (ASC1, NLRP3, and Caspase 1) in resting as well as in LPS induced macrophages were unaltered in control vs. Miltefosine treated cells. LPS mediated induction in protein levels of NLRP3 was also not altered by Miltefosine treatment. The levels of pro IL-1β were lower in Miltefosine treated cells as compared to control cells but the LPS mediated induction was still intact. The mature IL-1β is released via Gasdermin D pores[11], but Miltefosine treatment did not alter the levels of Gasdermin D. The intriguing question raised by these data is that if all inflammasome components are present and more or less equally induced by LPS in control vs. Miltefosine treated macrophages, why the Nlrp3 inflammasome is not assembled in Miltefosin treated cells. Mitochondria do play an essential role in activating Nlrp3 inflammasome[41, 49]. Miltefosine treated cells showed reduced levels of ROS upon LPS treatment (***Fig. 7E, F***). Based on our data, we speculate that Miltefosine treated macrophages failed to assemble Nlrp3 inflammasome due to lower levels of oxidative stress and efficient removal of damaged mitochondria (mitophagy), thus blocking Nlrp3 inflammasome assembly. Recent studies have shown that a serine threonine kinase Nek7 binds directly to Nlrp3 to promote inflammasome assembly, though kinase activity of Nek7 is not required for this function[50-52]. Nek7-Nlrp3 interaction is required for Nlrp3 inflammasome assembly and is dependent on potassium efflux [51]. Though Nek7 and Nlrp3 protein levels are not affected by Miltefosine treatment, Miltefosine can prevent potassium efflux and inhibit Nek7-Nlrp3 binding and prevent Nlrp3 inflammasome assembly.

Based on our data, Miltefosine or compounds with similar activities can be combined with statins to prevent CVD. Given the effects of Miltefosine on NLRP3 inflammasome pathway and IL-1β release, it may also serve as potential therapeutic for metabolic diseases where Nlrp3 inflammasome is hyper activated; such as diabetes, non-alcoholic fatty liver disease (NAFLD) and high fat diet induced inflammation. Further work is required to fully understand the

underlying molecular mechanisms responsible for spectrum of Miltefosine' s actions on macrophage cellular functions.

Material and Methods

Cell culture and reagents: All cell culture incubations were performed at 37ºC, unless otherwise indicated, in a humidified 5% CO_2 incubator. The growth media was Dulbecco's Modified Eagle Medium (DMEM) with 10% fetal calf serum, 100 µg/mL penicillin, 100 µg/mL streptavidin. Drugs were added to growth media at indicated concentrations and an equivalent amount of vehicle was added as control. Miltefosine, 18:1 NBD-PS, perifosine, edelfosine were obtained from Avanti polar and Echelon biosciences, methyl-β-cyclodextrin is obtained from Sigma Aldrich. ^{3}H-cholestreol (NET13900) was obtained from Perkin- Elmer. The primers for RT-PCR were obtained from ThermoFisher and siRNAs were obtained from Dharmacon (see supplementary material and methods). The RAW264.7 cells were from ATCC. Mifepristone ABCA1-inducible BHK cells, as previously described were obtained from Chongren Tang, University of Washington[53]. Mifepristone SR-BI-inducible BHK cells, as previously described[54], were obtained from Alan Remaley, NIH[54]. ABCA1-GFP and the mutant isoform stably transfected HEK cells were as previously described[55]. Primary and secondary antibodies were purchased from various sources (see supplementary material and methods).

Mice

WT C57BL6 or C57BL6 *ApoE*$^{-/-}$ mice were maintained on chow diet and sacrificed at 16 weeks of age. Femurs were collected to isolate and culture bone marrow macrophages using conditioned L-cell media.

Isolation of total RNA from BMM cell pellets

Total RNA was isolated from cell pellets using the RNeasy Mini Kit (Qiagen, Valencia, CA), following the manufacturer's protocol. On-column digestion with RNase-free DNase (Qiagen, Valencia, CA) was performed to remove genomic DNA. The qRT-pCR assays were performed using TaqMan reagent from ThermoFisher following the manufacturer's protocol.

Cholesterol efflux assay: The HEK293-Abca1-GFP cells, BHK cells, or RAW 264.7 murine macrophages were plated in 24-well plates at a density of 300-400,000 cells per well. The cells were labeled with 3H cholesterol in 1% FBS in DMEM for 24h. The labeled cells were induced for ABCA1 expression for 16h with 0.3 mM 8Br-cAMP (for RAW264.7 cells) or with 10nM Mifepristone (for BHK cells). Inducers were included in the media during subsequent assays. ABCA1 expression was confirmed by western blot using the AC10 antibody. The cells were washed with serum free media and chased for indicated time period in serum-free DMEM in the presence or absence of indicated treatments. The radioactivity in the chase media was determined after brief centrifugation to pellet any residual debris. Radioactivity in the cells was determined by extraction in hexane:isopropanol (3:2) with the solvent evaporated in a scintillation vial prior to counting. The percent cholesterol efflux was calculated as 100 × (medium dpm) / (medium dpm + cell dpm).

Lipid-Raft quantification: RAW cells were treated with 7.5 µg/ml Miltefosine at 37ºC for 16h. For imaging, cells were treated with 1 µg/ml Alexa647-CT-B labeled cells and images were captured using epifluorescent microscopy. For quantification, the cells were washed twice with PBS and gently scraped in 1.5 ml PBS. The Alexa647-CT-B (1µl of 1.5 mg/ml stock in PBS was added to 1.5 ml cells) was added at final concentration of 1 µg/ml to cells in 5 ml polystyrene round-bottom tubes (12 X 75 mm). The samples were subjected to Flow analysis with BD Biosciences LSRII cytometer using laser (Alexa 647 (Red) Ex: 639, Em: 650-670, Filter 660/20) and data was analyzed by Flowjo software.

Total/FC measurements: RAW264.7 cells grown in 12-well plates were loaded with 50 µg/ml cholesterol-CD or with 100 µg/ml AcLDL for 16 h at 37 °C with or without 2 µg/ml ACATi

treatment for 2h. The total cholesterol and free cholesterol levels were determined by using enzymatic assay as described earlier[33]. Detailed protocol is described in SI.

ApoA1 lipid solubilization assay: DMPC dissolved in chloroform:methanol (2:1, v:v) plus 5 mole% Miltefosine was dried in a stream of nitrogen onto the sides of a glass culture tube and kept in vacuum overnight. The DMPC film was rehydrated at 5 mg/mL in PBS by extensive vortexing and alternating freeze/thaw in a dry ice/ethanol and 37°C water bath. The resulting DMPC-DPH multi-lamellar vesicles (MLV)s were warmed to 37°C and extruded 11 times through a polycarbonate membrane using a mini-extruder (Avanti Polar Lipids) to derive large unilamellar vesicles (LUVs) of 100 nm diameter. 20 µg of these MLVs in Tris-buffered saline-EDTA (pH7.5) were incubated with 1 µg of human apoAI at 25 ºC in a final volume of 200 µl. MLV solubilization by human apoAI was monitored by measuring sample turbidity (absorbance) at 325 nm using a plate spectrophotometer.

Flow-Cytometry analysis: To measure cell surface PS, cells were cultured in 6 well plates in growth media, washed twice with PBS, and were resuspended in 500 µl Annexin V binding buffer plus 1 µl of Annexin V-Cy5 (Biovision). The samples were incubated at room temperature for 5 minutes in the dark. Flow cytometry analysis was performed using a BD Biosciences LSRFortessa cytometer using a 639 nm excitation laser and emission at 650-670 nm; and, data was analyzed using Flowjo software. To measure the inward translocation of various NBD labeled PS, RAW cells were incubated with phenol-red free DMEM containing 25 µM NBD-PS for 15 min at RT. The media was then replaced with PBS. The cells were gently scraped and were subjected to flow cytometry analysis first without sodium dithionite to calculate total NBD fluorescence, and then 5 min after the addition of 30 µl of a freshly prepared 1M sodium dithionite solution to determine the fraction of the signal resistant to quenching (translocated signal). Flow cytometry analysis was performed as above using a 488

nm laser for excitation and emission at 505-525 nm. To measure cell surface lipid rafts, a flow-cytometry based CTB Alexa 647-GM1 binding assay was used as described previously [23]. RAW cells were treated with either DMSO vehicle or 7.5 µM Miltefosine (16 hr pretreatment) at 37ºC. These cells were then washed twice with PBS and gently scraped in 1.5 ml PBS. Alexa 647-CTB was added at final concentration of 1 µg/ml and incubated for 1 min prior to flow cytometry as described above using a 639 nm excitation laser and emission at 650-670 nm.

Western blotting

RAW264.7 cells or BMDMs were grown treated as indicated. The PBS-washed cell pellet was lysed in 200 µL of NP40 lysis buffer. After discarding the nuclear pellet, the protein concentration was determined using the BCA protein assay (Pierce). 10-50 µg of cell protein samples were run on Novex 4-20% Tris-Glycine Gels (Invitrogen) and transferred onto polyvinylidene fluoride membranes (Invitrogen). Blots were incubated sequentially with 1:1000 rabbit polyclonal antibody raised against Nlrp3 (cell signaling), or 1:5000 rabbit polyclonal antibody raised against P-AMPK (cell signaling), or 1:1000 rabbit polyclonal antibody raised against IL1-b (cell signaling), 1:1000 rabbit polyclonal antibody raised against Gasdermin D, 1:1000 rabbit polyclonal antibody raised against ASC1. The signal was detected with an enhanced chemiluminescent substrate (Pierce). For LC3 western blot, RAW264.7 cells were incubated with or without 7.5 µM Miltefosine for 16 h, indicated wells received 30 µM chloroquine during the last 2 h of incubation. Blots were sequentially incubated with 1:1,000 rabbit polyclonal antibody raised against LC3B and 1:10,000 horseradish peroxidase-conjugated goat anti-rabbit as described above. GAPDH was used as a loading control.

Indirect immunofluorescence/fluorescent microscopy

RAW264.7 cells or BMDMs were grown in 4-chamber slides in indicated growth media. Cells were washed with 1xPBS, fixed with paraformaldehyde, and then incubated with

permeabilization solution (1xPBS/0.2% Triton X-100) for 10 min at RT. Cells were washed with 1xPBS three times and blocked with normal goat serum (1xPBS/1%BSA/5% normal goat serum) at 37ºC for 30 min. The cells were probed with p62 antibody and Alexa 647 labeled secondary antibody. For LC3 staining, RAW264.7 cells were transfected with LC3-GFP (Addgene) using lipofectamine LTX according to manufacturer protocol (Life Technologies). Cells were treated with or without 7.5 μM Miltefosine for 16 h. For ASC1 staining, Bone marrow derived macrophages from WT C57BL6 or C57BL6 apoE$^{-/-}$ KO mice were treated ± 5 μM Miltefosine for 16 h or ± 1mM cyclodextrin for 2h. All images were captured using an Olympus IX51 inverted epifluorescent microscope, Olympus LUCPlanFl ×40/0.6 lens, with a Q-Image EXi aqua camera and Olympus cellSens Dimension version 1.7 software. Post-imaging processing was performed in Adobe Photoshop CS2.

Total and cell surface ABCA1 levels: RAW 267.4 cells were cultured in DMEM with 10% FBS and were treated with 300 μM 8Br-cAMP to induce ABCA1 for 16 hr. Cells were incubated with incubated with or without 7.5μM Miltefosine for 4h. The cells were then incubated for 30 minutes on ice with phosphate-buffered saline (PBS) containing 1 mg/mL sulfo-NHS-biotin (Pierce). The PBS-washed cell pellet was lysed in 200 μl of lysis buffer (150 mM sodium chloride, 5 mM EDTA, 50 mM Tris-phosphate pH 8.0, 1% NP40, and 10% protease inhibitor). Cell-surface ABCA1 was determined by purifying biotinylated proteins by overnight incubation of 250 ug of cell protein with 75 uL of UltraLink Plus Immobilized Streptavidin gel (Pierce) at 4°C. The beads were spun down, washed, and resuspended by boiling in 100 μl 1x NuPage LDS Sample buffer (Invitrogen) and 20 μg of total protein were run on NuPAGE 3-8% Tris-Acetate gels (Invitrogen) and transferred onto polyvinylidene fluoride membranes (Invitrogen). Blots were incubated sequentially with 1:500 mouse monoclonal antibody raised against ABCA1 (AC10) and 1:15 000 horseradish peroxidase-conjugated goat

anti-mouse secondary antibody (Biorad). The signal was detected with an enhanced chemiluminescent substrate (Pierce).

PIP2 cellular reporter assay: RAW264.7 macrophage cell lines stably transfected with 2PH-PLCδ-GFP plasmid was described earlier[32]. Live or fixed cells were visualized by epifluorescent microscopy. Images were taken using the same exposure time.

Statistical analyses: Data are shown as mean ± SD. Comparisons of 2 groups were performed by a 2-tailed t test, and comparisons of 3 or more groups were performed by ANOVA with Bonferroni posttest. All statistics were performed using Prism software (GraphPad).

Author Contributions

A.J.I., and H.L. performed the experiments. J.H. performed the PS translocation assay. G.B., and B. A. R., performed the liposome solubilization assays. J.D.S. provided help with data analysis. K. G. conceived of the project idea, designed and directed study, performed experiments, performed data analyses and drafted the manuscript. All authors critically reviewed the manuscript.

Acknowledgments

We thank Dr. Brian Ritchey for the technical assistance and Dr. Shuhui Wang Lorkowski for providing reagents. This research was supported by NIH grants R01 HL128268 and R01 HL130085R01/PO1 to J.D.S. and American Heart Association scientist development grant SDG25710128 to K.G.

References

1. Tabas, I. Macrophage death and defective inflammation resolution in atherosclerosis. *Nat Rev Immunol* **10**, 36-46 (2010).
2. Duewell, P. *et al.* NLRP3 inflammasomes are required for atherogenesis and activated by cholesterol crystals. *Nature* **464**, 1357-1361 (2010).
3. Razani, B. *et al.* Autophagy links inflammasomes to atherosclerotic progression. *Cell metabolism* **15**, 534-544 (2012).
4. Hansson, G.K. & Klareskog, L. Pulling down the plug on atherosclerosis: cooling down the inflammasome. *Nature medicine* **17**, 790-791 (2011).
5. Zheng, F., Xing, S., Gong, Z. & Xing, Q. NLRP3 inflammasomes show high expression in aorta of patients with atherosclerosis. *Heart Lung Circ* **22**, 746-750 (2013).
6. Stienstra, R. *et al.* Inflammasome is a central player in the induction of obesity and insulin resistance. *Proceedings of the National Academy of Sciences of the United States of America* **108**, 15324-15329 (2011).
7. Ridker, P.M. *et al.* Antiinflammatory Therapy with Canakinumab for Atherosclerotic Disease. *The New England journal of medicine* **377**, 1119-1131 (2017).
8. Liu, X. *et al.* Inflammasome-activated gasdermin D causes pyroptosis by forming membrane pores. *Nature* **535**, 153-158 (2016).
9. Kayagaki, N. *et al.* Caspase-11 cleaves gasdermin D for non-canonical inflammasome signalling. *Nature* **526**, 666-671 (2015).
10. Ding, J. *et al.* Pore-forming activity and structural autoinhibition of the gasdermin family. *Nature* **535**, 111-116 (2016).
11. Evavold, C.L. *et al.* The Pore-Forming Protein Gasdermin D Regulates Interleukin-1 Secretion from Living Macrophages. *Immunity* (2017).
12. Xu, X.H. *et al.* Toll-like receptor-4 is expressed by macrophages in murine and human lipid-rich atherosclerotic plaques and upregulated by oxidized LDL. *Circulation* **104**, 3103-3108 (2001).
13. Liao, X. *et al.* Macrophage autophagy plays a protective role in advanced atherosclerosis. *Cell metabolism* **15**, 545-553 (2012).
14. Ouimet, M. *et al.* Autophagy regulates cholesterol efflux from macrophage foam cells via lysosomal acid lipase. *Cell metabolism* **13**, 655-667 (2011).
15. Sergin, I. & Razani, B. Self-eating in the plaque: what macrophage autophagy reveals about atherosclerosis. *Trends in endocrinology and metabolism: TEM* **25**, 225-234 (2014).
16. Khera, A.V. *et al.* Cholesterol efflux capacity, high-density lipoprotein function, and atherosclerosis. *The New England journal of medicine* **364**, 127-135 (2011).
17. Wang, X. *et al.* Macrophage ABCA1 and ABCG1, but not SR-BI, promote macrophage reverse cholesterol transport in vivo. *The Journal of clinical investigation* **117**, 2216-2224 (2007).
18. Yvan-Charvet, L., Wang, N. & Tall, A.R. Role of HDL, ABCA1, and ABCG1 transporters in cholesterol efflux and immune responses. *Arteriosclerosis, thrombosis, and vascular biology* **30**, 139-143 (2010).
19. Oram, J.F. ABCA1 as a New Therapeutic Target for Treating Cardiovascular Disease. *Drug news & perspectives* **15**, 24-28 (2002).
20. Oram, J.F. HDL apolipoproteins and ABCA1: partners in the removal of excess cellular cholesterol. *Arteriosclerosis, thrombosis, and vascular biology* **23**, 720-727 (2003).

21. Zhu, X. *et al.* Macrophage ABCA1 reduces MyD88-dependent Toll-like receptor trafficking to lipid rafts by reduction of lipid raft cholesterol. *Journal of lipid research* **51**, 3196-3206 (2010).
22. Rios-Marco, P., Jimenez-Lopez, J.M., Marco, C., Segovia, J.L. & Carrasco, M.P. Antitumoral alkylphospholipids induce cholesterol efflux from the plasma membrane in HepG2 cells. *J Pharmacol Exp Ther* **336**, 866-873 (2011).
23. Gulshan, K., Brubaker, G., Wang, S., Hazen, S.L. & Smith, J.D. Sphingomyelin Depletion Impairs Anionic Phospholipid Inward Translocation and Induces Cholesterol Efflux. *The Journal of biological chemistry* (2013).
24. Fukuda, M. *et al.* Conformational change of apolipoprotein A-I and HDL formation from model membranes under intracellular acidic conditions. *Journal of lipid research* **49**, 2419-2426 (2008).
25. Simons, K. & Toomre, D. Lipid rafts and signal transduction. *Nature reviews. Molecular cell biology* **1**, 31-39 (2000).
26. Landry, Y.D. *et al.* ATP-binding cassette transporter A1 expression disrupts raft membrane microdomains through its ATPase-related functions. *The Journal of biological chemistry* **281**, 36091-36101 (2006).
27. Yvan-Charvet, L. *et al.* Increased inflammatory gene expression in ABC transporter-deficient macrophages: free cholesterol accumulation, increased signaling via toll-like receptors, and neutrophil infiltration of atherosclerotic lesions. *Circulation* **118**, 1837-1847 (2008).
28. van der Luit, A.H. *et al.* A new class of anticancer alkylphospholipids uses lipid rafts as membrane gateways to induce apoptosis in lymphoma cells. *Mol Cancer Ther* **6**, 2337-2345 (2007).
29. Weller, K. *et al.* Miltefosine inhibits human mast cell activation and mediator release both in vitro and in vivo. *J Invest Dermatol* **129**, 496-498 (2009).
30. Jimenez-Lopez, J.M., Rios-Marco, P., Marco, C., Segovia, J.L. & Carrasco, M.P. Alterations in the homeostasis of phospholipids and cholesterol by antitumor alkylphospholipids. *Lipids in health and disease* **9**, 33 (2010).
31. Alder-Baerens, N. *et al.* Headgroup-specific exposure of phospholipids in ABCA1-expressing cells. *The Journal of biological chemistry* **280**, 26321-26329 (2005).
32. Gulshan, K. *et al.* PI(4,5)P2 Is Translocated by ABCA1 to the Cell Surface Where It Mediates Apolipoprotein A1 Binding and Nascent HDL Assembly. *Circulation research* **119**, 827-838 (2016).
33. Robinet, P., Wang, Z., Hazen, S.L. & Smith, J.D. A simple and sensitive enzymatic method for cholesterol quantification in macrophages and foam cells. *Journal of lipid research* **51**, 3364-3369 (2010).
34. Michelsen, K.S. *et al.* Lack of Toll-like receptor 4 or myeloid differentiation factor 88 reduces atherosclerosis and alters plaque phenotype in mice deficient in apolipoprotein E. *Proceedings of the National Academy of Sciences of the United States of America* **101**, 10679-10684 (2004).
35. Ito, A. *et al.* LXRs link metabolism to inflammation through Abca1-dependent regulation of membrane composition and TLR signaling. *eLife* **4**, e08009 (2015).
36. Dong, F., Mo, Z., Eid, W., Courtney, K.C. & Zha, X. Akt inhibition promotes ABCA1-mediated cholesterol efflux to ApoA-I through suppressing mTORC1. *PloS one* **9**, e113789 (2014).

37. Janoudi, A., Shamoun, F.E., Kalavakunta, J.K. & Abela, G.S. Cholesterol crystal induced arterial inflammation and destabilization of atherosclerotic plaque. *European heart journal* **37**, 1959-1967 (2016).
38. Juliana, C. *et al.* Non-transcriptional priming and deubiquitination regulate NLRP3 inflammasome activation. *The Journal of biological chemistry* **287**, 36617-36622 (2012).
39. Westerterp, M. *et al.* Deficiency of ATP-Binding Cassette Transporters A1 and G1 in Macrophages Increases Inflammation and Accelerates Atherosclerosis in Mice. *Circulation research* **112**, 1456-1465 (2013).
40. Westerterp, M. *et al.* Cholesterol Accumulation in Dendritic Cells Links the Inflammasome to Acquired Immunity. *Cell metabolism* **25**, 1294-1304 e1296 (2017).
41. Heid, M.E. *et al.* Mitochondrial reactive oxygen species induces NLRP3-dependent lysosomal damage and inflammasome activation. *Journal of immunology* **191**, 5230-5238 (2013).
42. Iyer, S.S. *et al.* Mitochondrial cardiolipin is required for Nlrp3 inflammasome activation. *Immunity* **39**, 311-323 (2013).
43. Linam, W.M. *et al.* Successful treatment of an adolescent with Naegleria fowleri primary amebic meningoencephalitis. *Pediatrics* **135**, e744-748 (2015).
44. Rios-Marco, P., Marco, C., Cueto, F.J., Carrasco, M.P. & Jimenez-Lopez, J.M. Pleiotropic effects of antitumour alkylphospholipids on cholesterol transport and metabolism. *Exp Cell Res* **340**, 81-90 (2016).
45. Nandi, S. *et al.* ABCA1-mediated cholesterol efflux generates microparticles in addition to HDL through processes governed by membrane rigidity. *Journal of lipid research* **50**, 456-466 (2009).
46. Pownall, H. *et al.* Kinetics and mechanism of association of human plasma apolipoproteins with dimyristoylphosphatidylcholine: effect of protein structure and lipid clusters on reaction rates. *Biochemistry* **20**, 6630-6635 (1981).
47. van Hout, G.P. *et al.* The selective NLRP3-inflammasome inhibitor MCC950 reduces infarct size and preserves cardiac function in a pig model of myocardial infarction. *European heart journal* **38**, 828-836 (2017).
48. van der Heijden, T. *et al.* NLRP3 Inflammasome Inhibition by MCC950 Reduces Atherosclerotic Lesion Development in Apolipoprotein E-Deficient Mice-Brief Report. *Arteriosclerosis, thrombosis, and vascular biology* **37**, 1457-1461 (2017).
49. Zhou, R., Tardivel, A., Thorens, B., Choi, I. & Tschopp, J. Thioredoxin-interacting protein links oxidative stress to inflammasome activation. *Nature immunology* **11**, 136-140 (2010).
50. Schmid-Burgk, J.L. *et al.* A Genome-wide CRISPR (Clustered Regularly Interspaced Short Palindromic Repeats) Screen Identifies NEK7 as an Essential Component of NLRP3 Inflammasome Activation. *The Journal of biological chemistry* **291**, 103-109 (2016).
51. He, Y., Zeng, M.Y., Yang, D., Motro, B. & Nunez, G. NEK7 is an essential mediator of NLRP3 activation downstream of potassium efflux. *Nature* **530**, 354-357 (2016).
52. Shi, H. *et al.* NLRP3 activation and mitosis are mutually exclusive events coordinated by NEK7, a new inflammasome component. *Nature immunology* **17**, 250-258 (2016).
53. Vaughan, A.M. & Oram, J.F. ABCA1 redistributes membrane cholesterol independent of apolipoprotein interactions. *Journal of lipid research* **44**, 1373-1380 (2003).
54. Vickers, K.C., Palmisano, B.T., Shoucri, B.M., Shamburek, R.D. & Remaley, A.T. MicroRNAs are transported in plasma and delivered to recipient cells by high-density lipoproteins. *Nature cell biology* **13**, 423-433 (2011).

55. Wang, S., Gulshan, K., Brubaker, G., Hazen, S.L. & Smith, J.D. ABCA1 mediates unfolding of apolipoprotein AI N terminus on the cell surface before lipidation and release of nascent high-density lipoprotein. *Arteriosclerosis, thrombosis, and vascular biology* **33**, 1197-1205 (2013).

Figure Legends

Figure 1: A) Miltefosine increased Abca1 mediated cholesterol efflux. RAW264.7 murine macrophages were labeled with ^{3}H-cholesterol and pretreated with or without 8Br-cAMP to induce ABCA1 and chase was performed for 1h at 37^{o}C. Serum free DMEM was used as chase media containing either vehicle, 7.5 μM or 10μM Miltefosine. Cholesterol efflux from cells in ± Abca1 and ± Miltefosine conditions. Values are % cholesterol efflux mean ± SD, N=5, asterisks above the bars show p<0.0001 by ANOVA Bonferroni posttest, comparing control vs. control + Miltefosine, apoA1 vs apoA1 +Miltefosine, Abca1 vs. Abca1 +Miltefosine, and Abca1+apoA1 vs. Abca1+apoA1+ Miltefosine. N.S=non-significant ***B)*** Western blot analysis of total and cell-surface Abca1 from RAW264.7 cell extracts ± 7.5 μM Miltefosine for 4h. ***C)*** RAW macrophages ± Abca1 were treated ± 7.5 μM Miltefosine for 4 hrs at 37^{o}C and washed twice with serum free and phenol-red free DMEM, followed by incubation with Alexa 647 labeled apoA1 in serum free and phenol-red free media for 45 minutes at RT. apoA1 binding to cell membrane was determined by flow cytometry. Values are the mean±SD of the median fluorescence from 3 independent wells, asterisks above the bars show p<0.05, by ANOVA Bonferroni posttest. ***D)*** Miltefosine promoted apoA1 mediated DMPC MLVs solubilization. Liposomes were prepared with DMPC alone or DMPC:Miltefosine (5 mole %). DMPC MLV solubilization after incubation with apoA1 (100:1 lipid:apoA1 mole ratio) at 25^{o}C was determined by measuring turbidity at 325 nm. ***E)*** Miltefosine (5 mole %) promoted solubilization of MLVs composed of POPC:POPS:cholesterol (70:20:10 mole ratio) incubated with apoA1 (100:1 lipid:apoA1 mole ratio) at 25^{o}C, pH 5.0.

Figure 2. ***Miltefosine disrupts lipid-rafts and inhibits PS flip across plasma membrane.*** **A)** GM1 levels assessed by binding of cholera toxin B (CTB) in RAW macrophages ± 7.5 μM Miltefosine for 16h at 37^{o}C and washed twice with PBS, followed by incubation with 1 μg/ml cholera toxin B (CTB)-Alexa 647 for 5 min at 37^{o}C. Cells were washed with PBS and visualized via fluorescent microscopy at room temperature. ***B)*** For quantification of CTB binding, RAW cells treated ± 7.5 μM Miltefosine for 16h at 37^{o}C were washed with PBS and were gently scraped from wells in PBS. 1 μg/ml Alexa 647 labeled CTB was added to cells and incubated for 1 min before subjecting to flow cytometry analysis. Values are the mean±SD of the median fluorescence from 3 independent wells, asterisks above the bars show p<0.01, by ANOVA Bonferroni posttest. ***C)*** Miltefosine increased cell surface PS. RAW macrophages were incubated with or without 8Br-cAMP to induce ABCA1 and ± 7.5 μM Miltefosine for 16 hrs. PS exposure was determined by flow cytometry via Annexin V binding. Values are the mean±SD of the median fluorescence from 3 independent wells, asterisks above the bars show p<0.01, by ANOVA Bonferroni posttest. ***D)*** Miltefosine impairs NBD- PS flip in RAW macrophages. Cells were treated with 7.5 μM Miltefosine or vehicle for 16 hrs. These cells were then incubated with 25 μM NBD-PS at RT for 15 min, washed with PBS, and subjected to fluorescent microscopy. ***E)*** Quantification of NBD-PS translocated inside the cells. RAW macrophages treated ± 7.5 μM Miltefosine for 16h at 37^{o}C, were incubated with 25 μM NBD-PS at 37^{o}C for 15 min in phenol red free DMEM. The cells were gently scraped and then subjected to flow cytometry analysis in the presence or absence of sodium dithionite as described in ***Material and methods*** section. Values are the % NBD-PS translocated into the cells, mean±SD of the median fluorescence from 3 independent wells, asterisks represent effect of Miltefosine in two-tailed t-tests; *, p<0.005.

Figure. 3. ***Miltefosine induces PIP2 delocalization from plasma membrane. A***) RAW264.7 cells stably transfected with 2X-PH-PLCeGFP reporter plasmid were treated ± 7.5 µM Miltefosine for 12h at 37ºC. The cells were washed with PBS and visualized under fluorescent microscope. ***B***) RAW264.7 cells stably transfected with 2X-PH-PLCeGFP reporter plasmid were treated ± 7.5 µM Miltefosine for 12h at 37ºC. The cells were fixed and stained with mouse anti beta- actin antibody and counterstained with Alexa 568 labeled goat anti-mouse secondary antibody, followed by visualization of cells under fluorescent microscope.

Figure. 4. ***Miltefosine induces autophagy.*** (*A*) RAW264.7 cells or LC3-GFP transfected RAW264.7 cells (lower panel) were treated with ± 7.5 µM Miltefosine for 16h at 37ºC, followed by staining with p62 antibody, using Alexa 568-conjugated secondary antibody to reveal bound antibody (red, upper panel). LC3-GFP protein (green) localization is shown in the lower panel. (*B*) RAW264.7 cells were treated with ± 7.5 µM Miltefosine for 16h at 37ºC. ***B)*** Autophagic flux was assessed in presence of chloroquine for the last 2 h of incubation. The amount of LC3-II was assessed by western blot and densitometry analysis. ***C)*** LC3-II levels were presented relative to GAPDH levels (N=3, mean±SD, **p<0.01, ***p<0.001 by ANOVA posttest). D) Cellular FC levels in RAW264.7 cells loaded with 100 µg/ml acetylated low-density lipoprotein (AcLDL), 100 µg/ml AcLDL+2 µg/ml ACATi or, 100 µg/ml AcLDL+ 7.5 µM Miltefosine +2 µg/ml ACATi (N=3, mean±SD, *p<0.5 vs. control **p<0.05 vs. control, by ANOVA posttest). ***E)*** Western blot analysis of phosphorylated form of AMPK from RAW264.7 cell extracts ± 7.5 µM Miltefosine for 4hrs or 16 hrs at 37ºC.

Figure. 5. Miltefosine dampened TLR4 signaling in bone marrow derived macrophages. A) Mouse BMDMs were treated with ± 5 µM Miltefosine for 16h at 37ºC. The cells were primed by incubation with ± 1mg/ml LPS at 37ºC for 4hrs, followed by cell extract preparation and western blot analysis using Phospho-AMPK antibody. GAPDH was used as loading control. ***B)*** BMDMs were treated with ± 5 µM Miltefosine for 16h at 37ºC. NF-kB localization was determined by staining with anti-NF-kB primary antibody and Alexa 568 labeled rabbit secondary antibody. ***C)*** Mouse BMDMs were treated with ± 5 µM Miltefosine for 16h at 37ºC. The cells were primed by incubation with ± 1mg/ml LPS at 37ºC for 4hrs, followed by mRNA preparation and qRT-PCR analysis of pro-IL-1 transcript with actin used as control transcript (N=6, mean ± SD). asterisks represent effect of Miltefosine in two-tailed t-tests; *, p<0.01. ***D)*** Mouse BMDMs were treated with ± 5 µM Miltefosine for 16h at 37ºC. The cells were primed by incubation with ± 1mg/ml LPS at 37ºC for 4hrs, followed by cell extract preparation and western blot analysis using IL1-β antibody. GAPDH was used as loading control.

Figure. 6. Miltefosine inhibited Nlrp3 inflammasome assembly and IL-1β release. A) Mouse BMDMs cultured in conditioned L-cell media were treated with ± 5 µM Miltefosine for 16h at 37ºC. The cells were primed by incubation with ± 1µg/ml LPS in conditioned L-cell media at 37ºC and induced for Nlrp3 inflammasome assembly by incubation with 1mM ATP for 20 min in DMEM. Cells were fixed with 100% ethanol and stained with anti-ASC1 antibody and Alexa-568 labeled rabbit secondary antibody, followed by epifluorescent microscopy. DAPI was used as counterstain to visualize nucleus ***B)*** Quantification of ASC1 speck formation in control vs. Miltefosine treated cells. Only DAPI +ve cells were used for counting. ***C)*** The IL-1β ELISA of media collected from cells treated with ± 5 µM Miltefosine for 16h at 37ºC and

induced for Nlrp3 inflammasome by LPS priming and ATP incubation. ***D)*** Mouse BMDMs were treated with ± 5 µM Miltefosine for 16h at 37ºC. The cells were primed by incubation with ± 1mg/ml LPS at 37ºC for 4hrs, followed by mRNA preparation and qRT-PCR analysis of NLRP3, GsdmD and caspase 1. Actin was used as control transcript (N=6, mean ± SD). asterisks represent effect of Miltefosine in two-tailed t-tests; *, p<0.01. Mouse BMDMs were treated with ± 5 µM Miltefosine for 16h at 37ºC, incubated with ± 1mg/ml LPS at 37ºC for 4hrs, followed by ± 1mM ATP incubation for 20 min. Cells extracts were prepared and western blot analysis was performed for Nlrp3 (***E***), Asc1 (***F***), and Caspase 1 (***G***). GAPDH was used as loading control.

Figure. 7*. Miltefosine specifically inhibits NLRP3 inflammasome and dampen LPS induced ROS generation. *A) Mouse BMDMs were treated with ± 5 µM Miltefosine ± 1.5 µM MCC950 for 16h at 37ºC. The cells were primed by incubation with ± 1mg/ml LPS at 37ºC and induced for Nlrp3 inflammasome assembly by incubation with 1mM ATP for 20 min, followed by IL-1β ELISA from collected media. ***B)*** Mouse BMDMs treated with ± 5 µM Miltefosine were primed with 1µg/ml LPS, followed by transfection with 2µg of poly (dA-dT) for 3h for inducing AIM2 inflammasome. The IL-1β ELISA was performed on collected media. ***C)*** Total cholesterol levels were determined in mouse BMDMs treated with ± 5 µM Miltefosine for 16h or 1mM cyclodextrin for 2h. ***D)*** Mouse BMDMs treated with ± 5 µM Miltefosine for 16h or 1mM cyclodextrin for 2h were primed by incubation with ± 1mg/ml LPS at 37ºC and induced for Nlrp3 inflammasome assembly by incubation with 1mM ATP for 20 min, followed by IL-1 ELISA from collected media. ***E)*** Mouse BMDMs treated with ± 5 µM Miltefosine were primed with 1µg/ml LPS, followed by 10 min incubation at 37ºC with 5µM Mitosox reagent. Cells were washed, counterstained with DAPI and imaged with epifluorescent microscopy. ***F)*** Flow-cytometry analysis showing quantification of MitoSox binding to cells in different conditions.

Figure 1

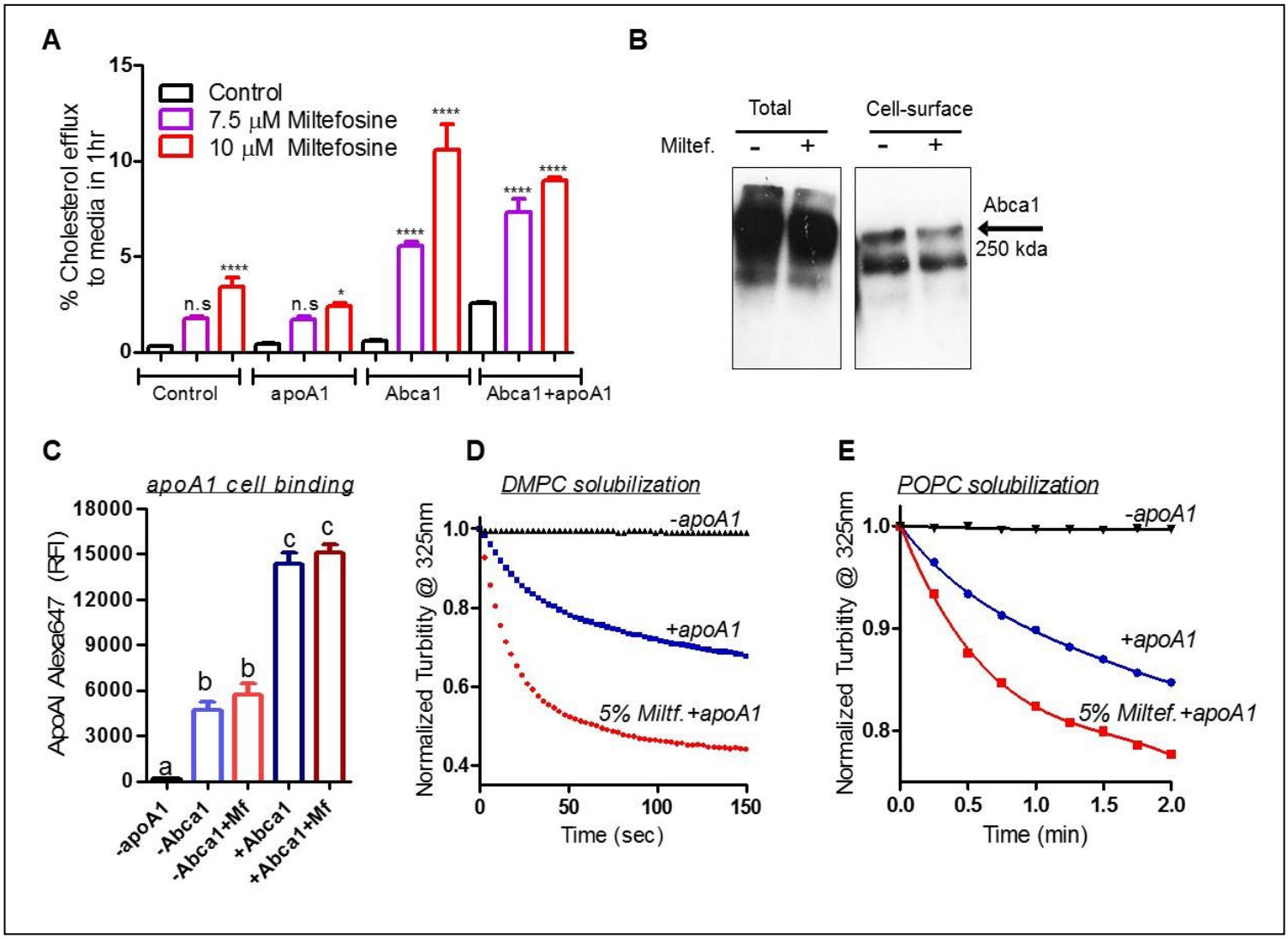

Figure 2

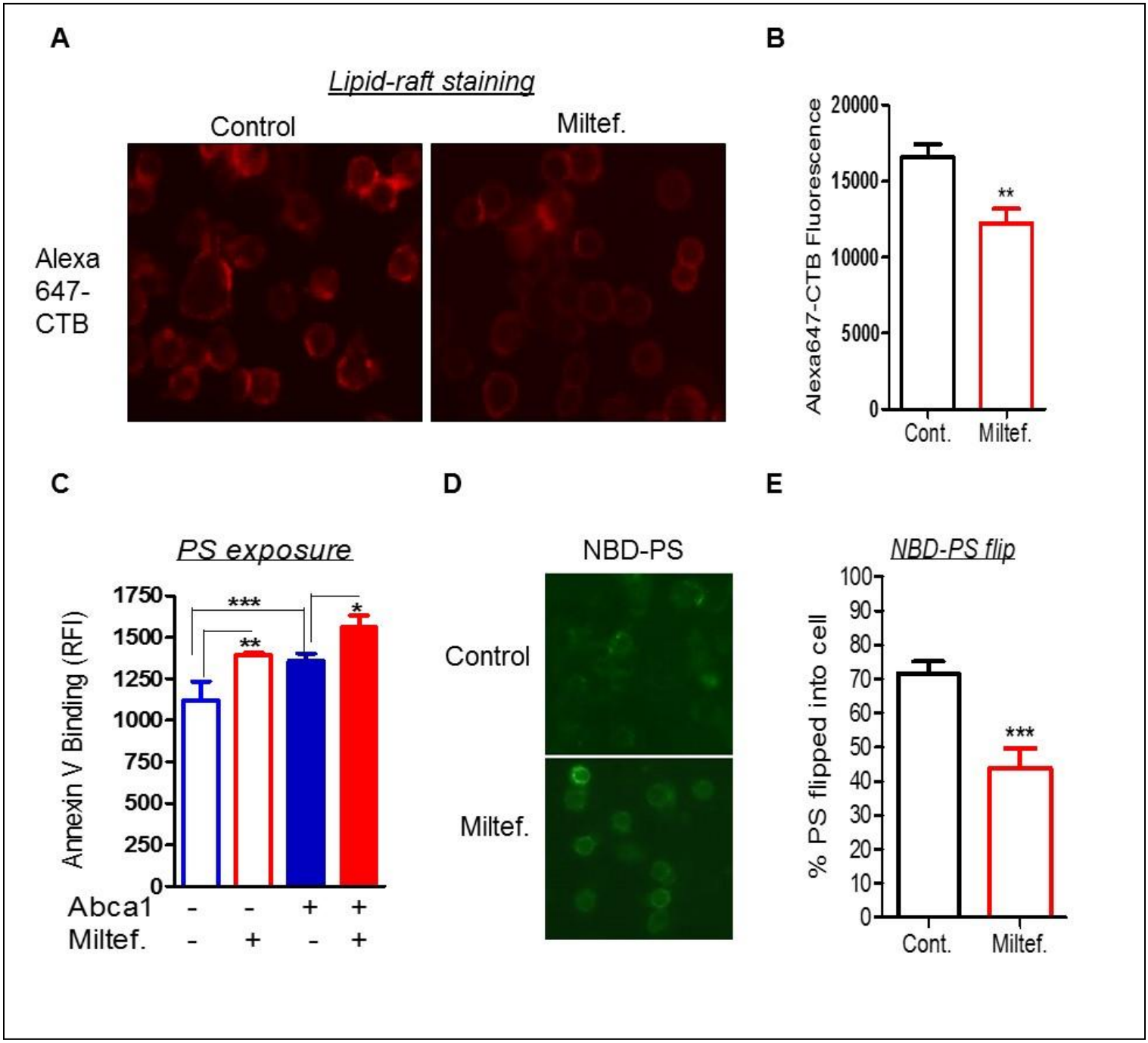

Figure 3

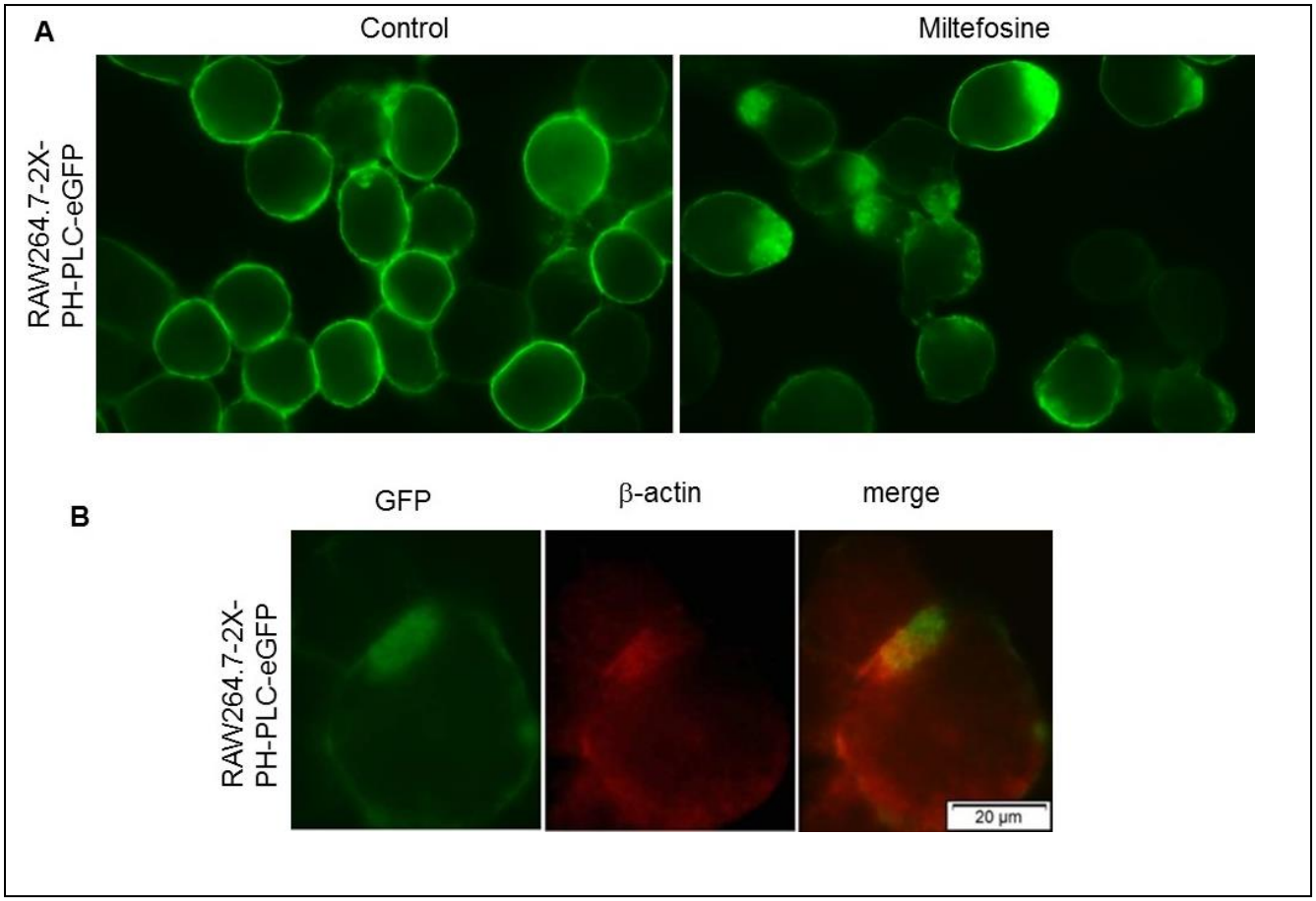

Figure 4

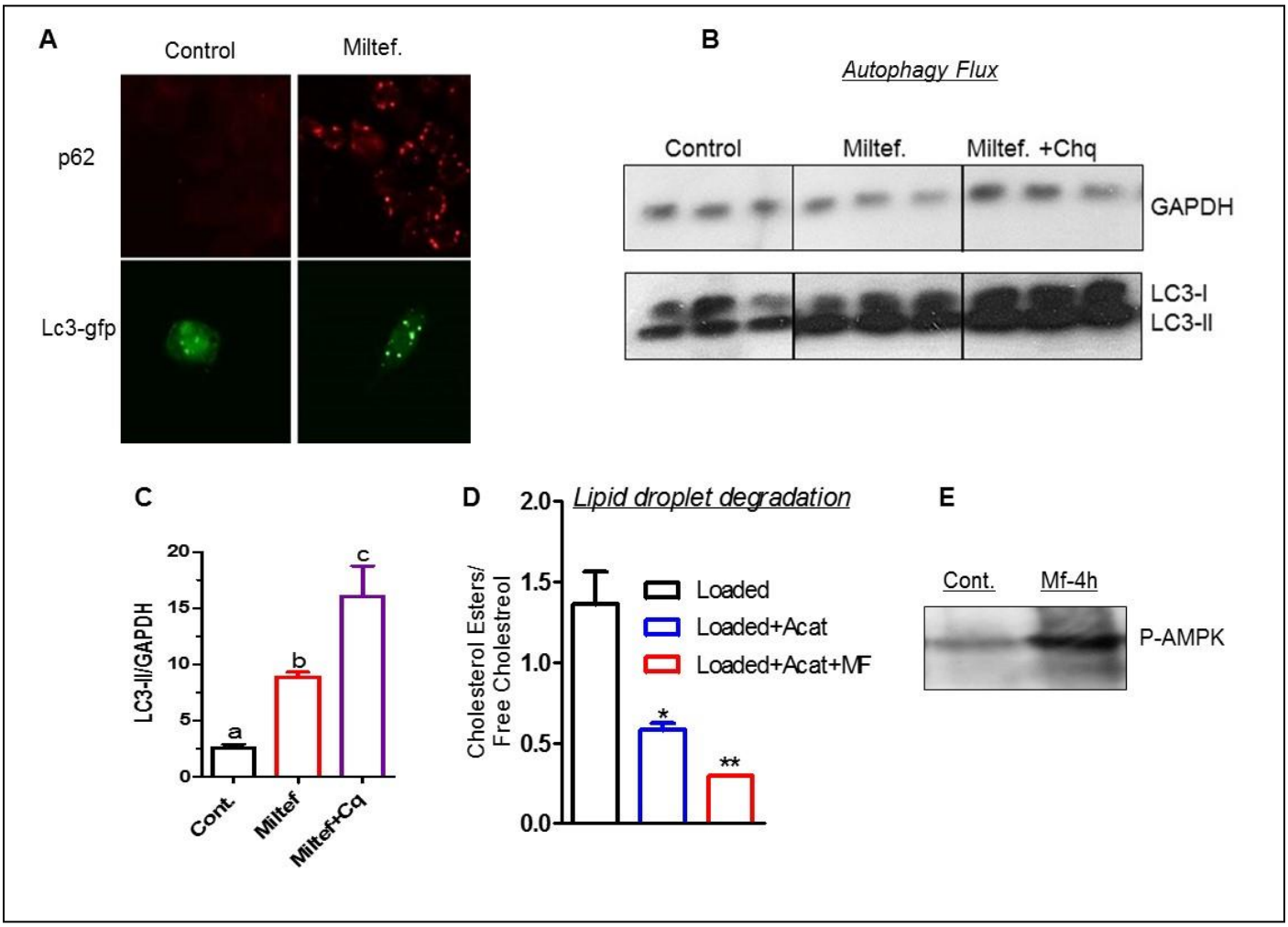

Figure 5

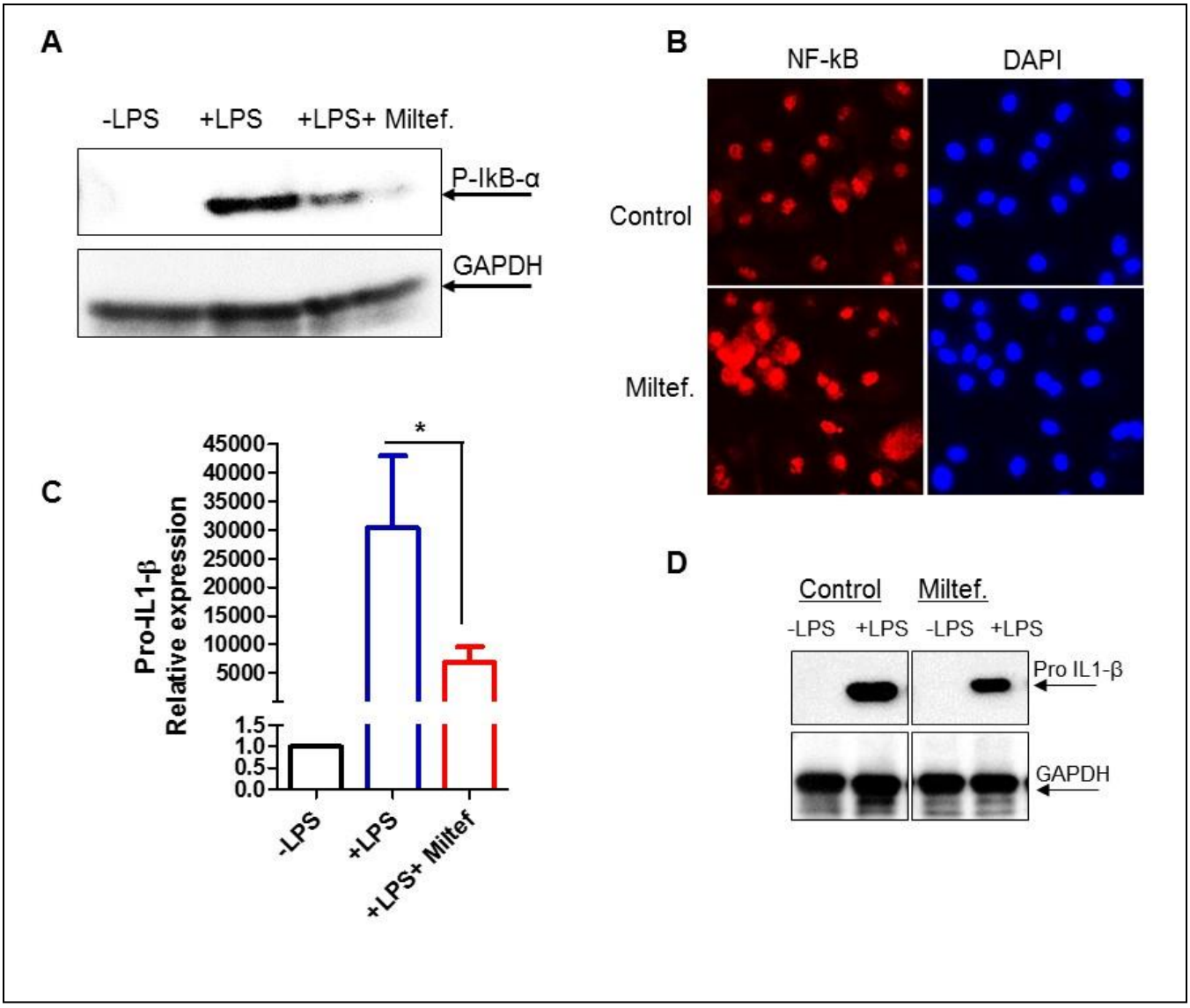

Figure 6

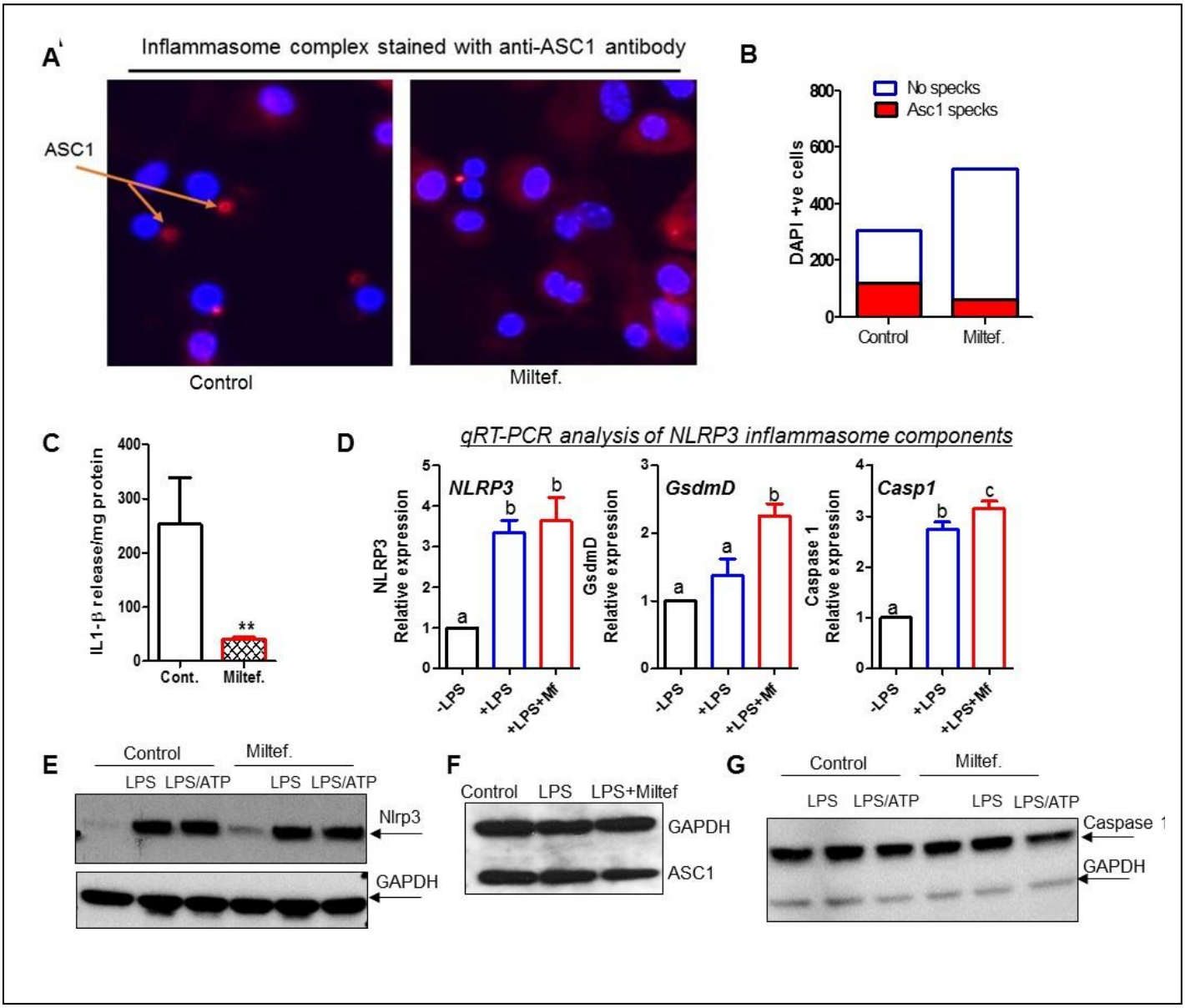

Figure 7

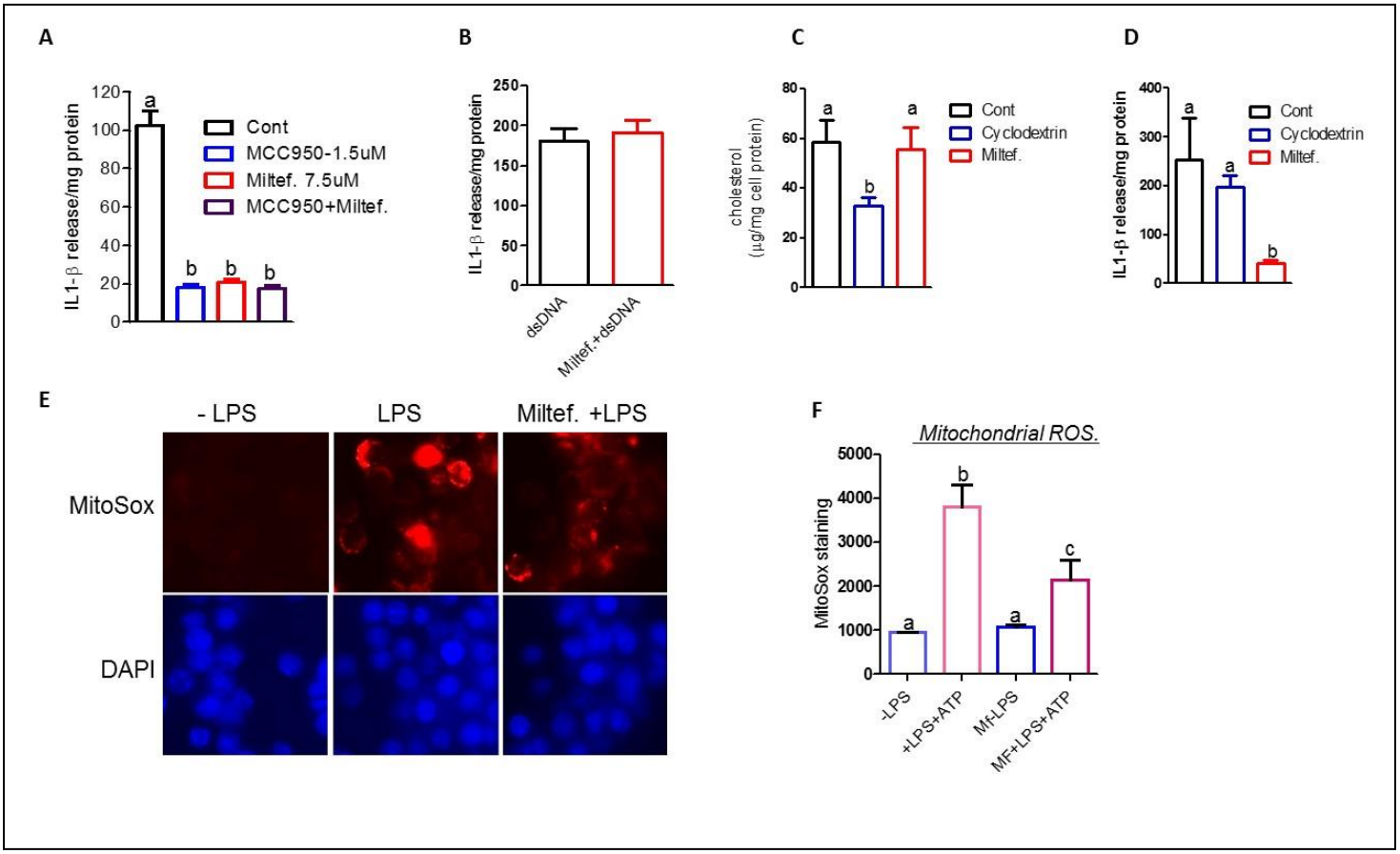

Supplementary Methods and Figures

Reagents: Antibodies:

GAPDH (14C10) Rabbit mAb- #2118

NLRP3 (D4D8T) Rabbit mAb- #15101

PIKBa (Ser32) (14D4) Rabbit mAb- #2859

NF-κB p65 (C22B4) Rabbit mAb- #4764

Phospho-AmpKa (The172) (40H9) Rabbit mAb- #2535S

AmpKa Ab- #2532S

GSDMD- #A10164

Pip4k2a- PA5-31141

Nek7- #Ab133514

qRT-PCR reagents and primers:

Qiagen	RNEasy MiniKit	74104
Biorad	iScript cDNA kit	170-8891
ThermoFisher	2x TaqMan	4304437
ThermoFisher	NIrp3	Mm00840904
	Casp1	Mm00438023
	Pycard	Mm00445747
	iL1B	Mm00434228
	Gsdmd	Mm00509958
	Actb	Mm02619580
Qiagen	Rnase-free Dnase set	79254

Supplementary Figures Legends:

Fig. S1: Miltefosine increased Abca1 mediated cholesterol efflux in HEK293 cells. HEK293 or HEK293-ABCA1 cells were labeled with ^{3}H-cholesterol. Serum free DMEM was used as chase media containing either vehicle, 7.5 uM or 10uM Miltefosine. Cholesterol efflux from cells in ± Abca1 and ± Miltefosine conditions. Values are % cholesterol efflux mean ± SD, N=5, asterisks above the bars show p<0.001 by ANOVA Bonferroni posttest.

Fig. S2: Miltefosine increased Abca1 mediated cholesterol efflux in BHK cells. BHK cells were labeled with ^{3}H-cholesterol. Cells were pretreated with or without 10nM Mifepristone to induce ABCA1 expression. Serum free DMEM was used as chase media containing either vehicle, 7.5 uM or 10uM Miltefosine. Cholesterol efflux from cells in ± Abca1 and ± Miltefosine conditions. Values are % cholesterol efflux mean ± SD, N=5, asterisks above the bars show p<0.001 by ANOVA Bonferroni posttest.

Fig. S3: Miltefosine increased Abca1 mediated cholesterol efflux. RAW264.7 murine macrophages were labeled with ^{3}H-cholesterol and pretreated with or without 8Br-cAMP to induce ABCA1 and chase was performed for 6h at 37^{o}C. Serum free DMEM was used as chase media containing either vehicle, 7.5 uM or 10uM Miltefosine. Cholesterol efflux from cells in ± Abca1 and ± Miltefosine conditions. Values are % cholesterol efflux mean ± SD, N=5, asterisks above the bars show p<0.001 by ANOVA Bonferroni posttest.

Fig. S4: Miltefosine analogues promoted apoA1 mediated DMPC MLVs solubilization. Liposomes were prepared with DMPC alone or DMPC:Miltefosine (5 mole %) or DMPC:Edelfosine (5 mole %) or DMPC:Perifosine (5 mole %). DMPC MLV solubilization after incubation with apoA1 (100:1 lipid:apoA1 mole ratio) at 25^{o}C was determined by measuring turbidity at 325 nm.

Fig. S5: Full image for Control BMDMs treated with LPS/ATP and stained with anti-ASC1 antibody.

Fig. S6: Full image for BMDMs treated with Miltefosine and LPS/ATP and stained with anti-ASC1 antibody.

Fig. S7: Western blot analysis of Gasdermin in bone marrow derived macrophages ±LPS/ATP and ±5 uM Miltefosine.

Fig. S8: Full image for BMDMs treated with cyclodextrin and LPS/ATP and stained with anti-ASC1 antibody

Fig. S1

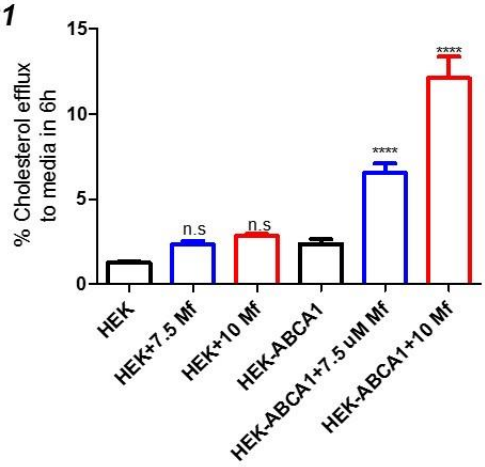

Fig. S2

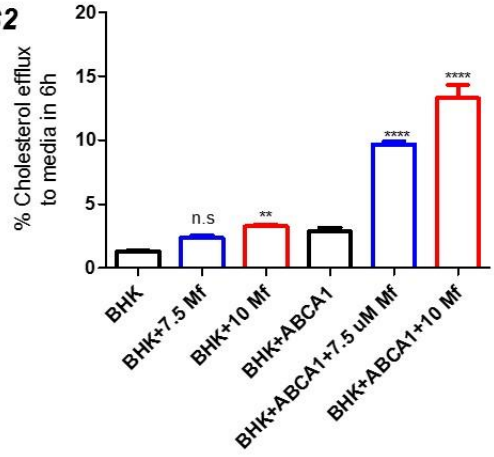

Fig. S3

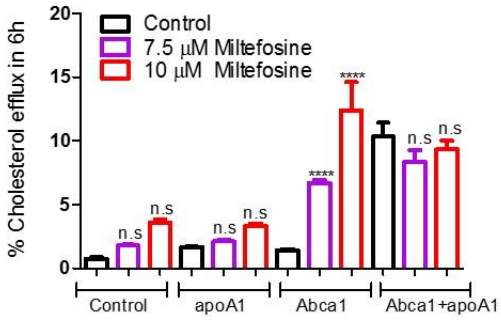

Fig. S4

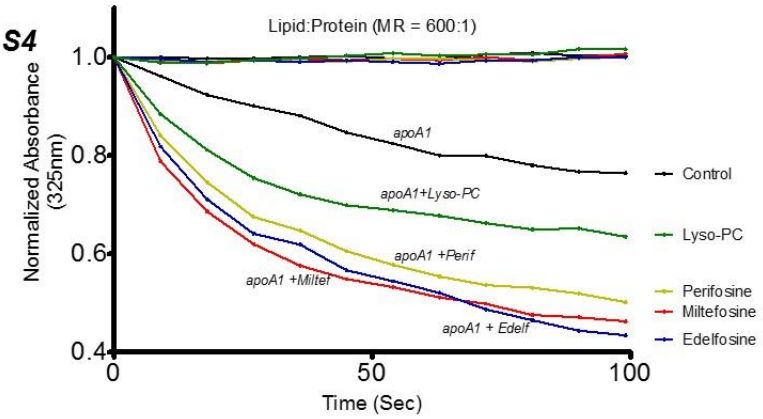

Fig. S5

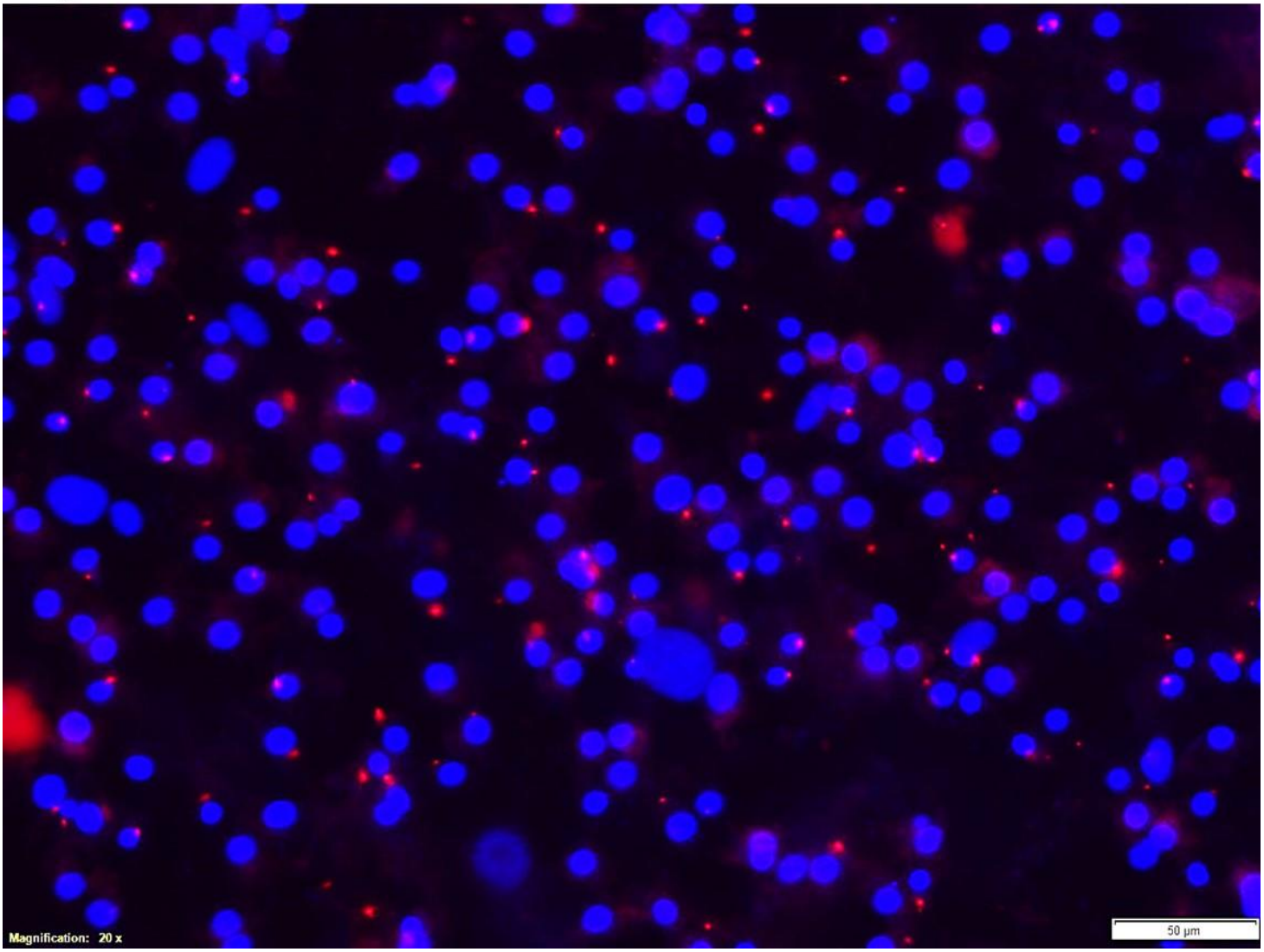

Fig. S6

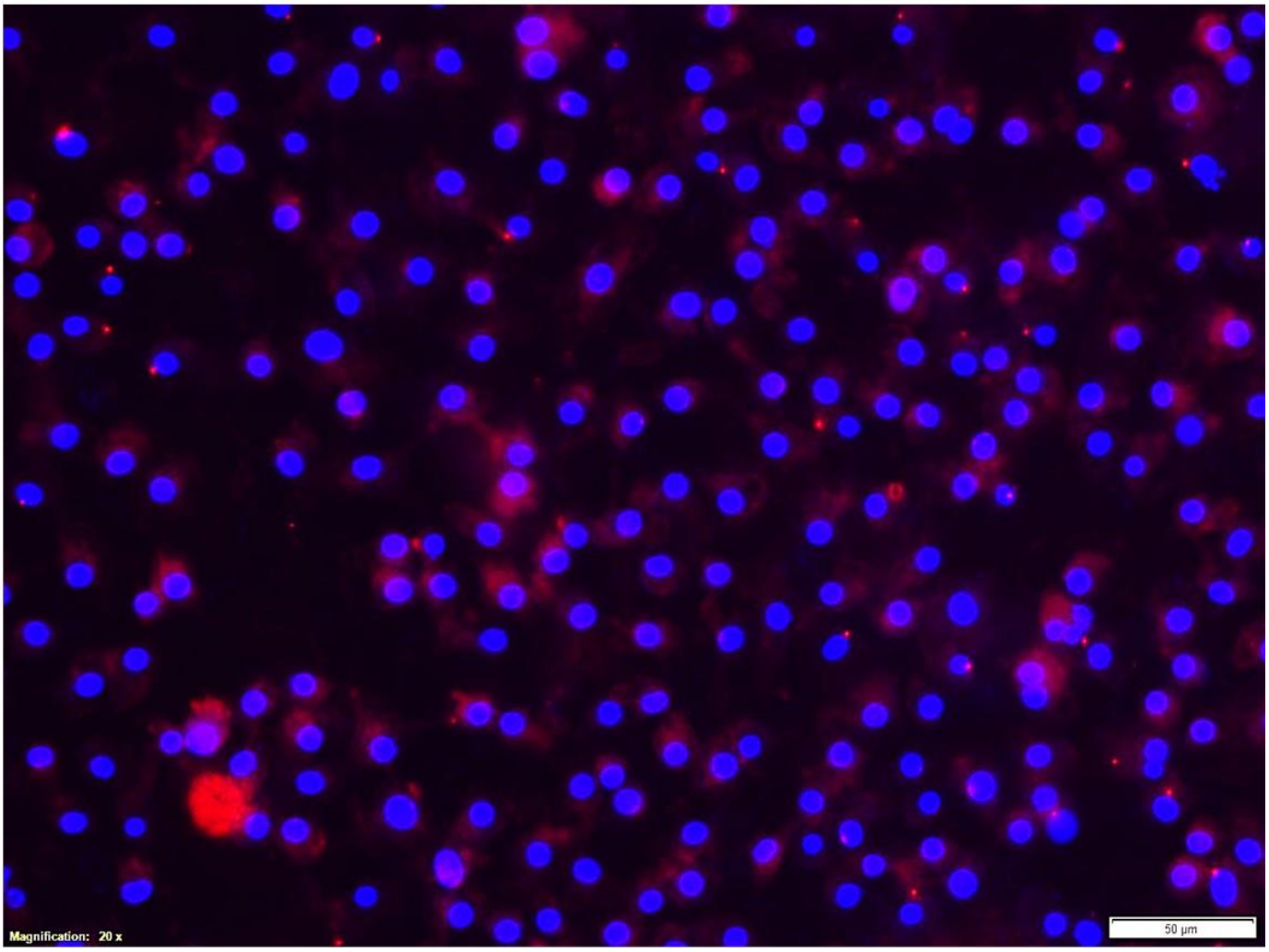

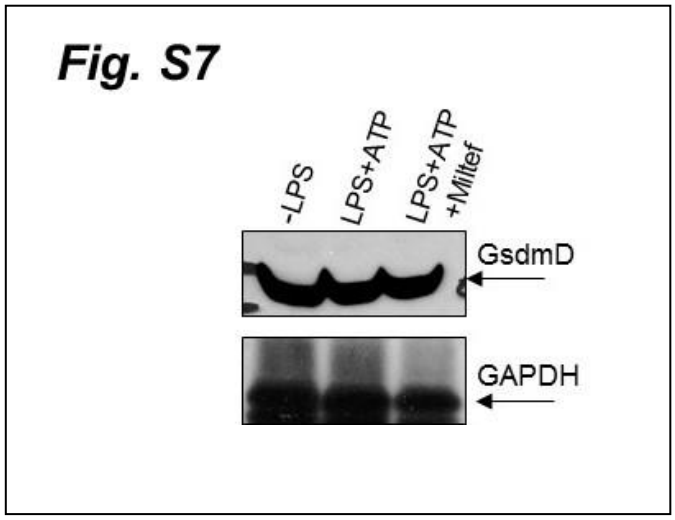

Fig. S8